



. . . « μ

μ

»



:

, 2012

2012/09



. . . « μ

μ

»



:

, 2012

2012/09

	μ	ii
Abstract		iii
1.		1
1.1	μ	1
1.2	μ	2
1.3		3
1.4	μ	7
1.5	μ μ	7
1.6	μ μ	8
2.	μ	12
2.1		12
2.1.1		12
2.1.2		17
2.2		20
2.2.1	μ μ	(thermoset).....	22
2.2.2	μo	(thermoplastic).....	25
2.2.3	μ , μ	26
2.2.4		29
2.2.5		30
3.		35
3.1	μ μ μ	-«hand lay-up».....	35
3.2	μ μ μ	-«prepreg lay-up».....	38
3.3	μ μ	- «bag molding».....	39
3.4	μ μ	-«autoclave processing».....	40
3.5	μ μ	- compression molding.....	41
3.6		- resin transfer molding (rtm).....	42
3.7	μ	- pultrusion.....	44
3.8		- filament winding.....	46
3.9	- μ	49
4.		52
4.1	μ μ	52
4.2	μ μ μ μ	Gfrp.....	58
4.3	μ pvc	-v: μ.....	61
4.4	μ μ μ	: μ.....	63
4.5	μ μ μ μ	68
4.6	μ μ μ	72
4.7		80
4.8	μ μ - μ	89
5.	/	98

NATIONAL TECHNICAL UNIVERSITY OF ATHENS
FACULTY OF CIVIL ENGINEERING
INSTITUTE OF STEEL STRUCTURES

DIPLOMA THESIS
2011/04

Modern developments in composite materials technology

Giannou Maria (supervised by Raftogiannis. I)

Abstract

One of the modern application fields in Engineering is, as known, the study of composite materials which are in continuous development over the last thirty years. The purpose of this master thesis is initially the study of their history and their structure, their advantageous properties compared to conventional materials and the advantages and disadvantages of the various production processes. Mostly though, selected modern developments in composite materials technology that open horizons for further research and applications in the future as well as for creating intelligent or smart structures / materials that can monitor their conditions, detect impending failure to control or treat damage and adapt to changing environments are presented in detail. So, through experimental and mathematical procedures and simulations, useful conclusions and reviews of the present data are drawn, which will definitely help in better understanding, improvement and application of complex and subsequently, smart materials.

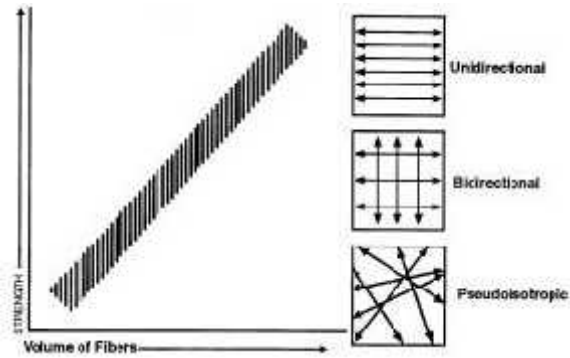
. μ , μ μ μ

1.

- μ
- μ (\dots (woven), stitched mat \dots)
- μ (\dots continuous strand mat-
- CSM)

- μ (\dots μ (chopped strand mat))
- μ (\dots oriented strand mat)

- μ
- μ
- μ



. 1.1: μ

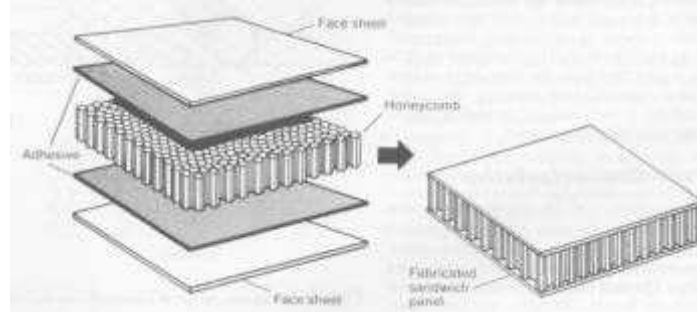
2. μ

- μ , μ μ μ , μ
- μ , μ

3.

- (\dots μ)
- (\dots μ μ) (intermingled borion carbon)

μ (bending stiffness)



. 1.4:

1.4

.1.6.

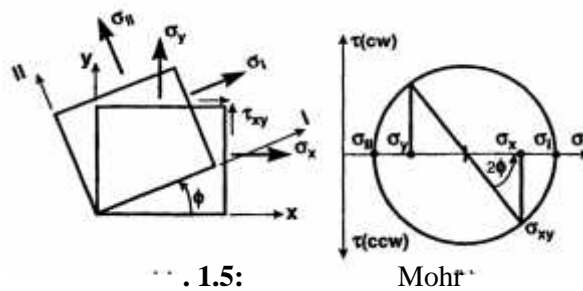
1.5

Mohr

$$\sigma_n = \frac{\sigma_x + \sigma_y}{2} + \left[\frac{(\sigma_x - \sigma_y)^2}{4} + \tau_{xy}^2 \right]^{1/2}$$

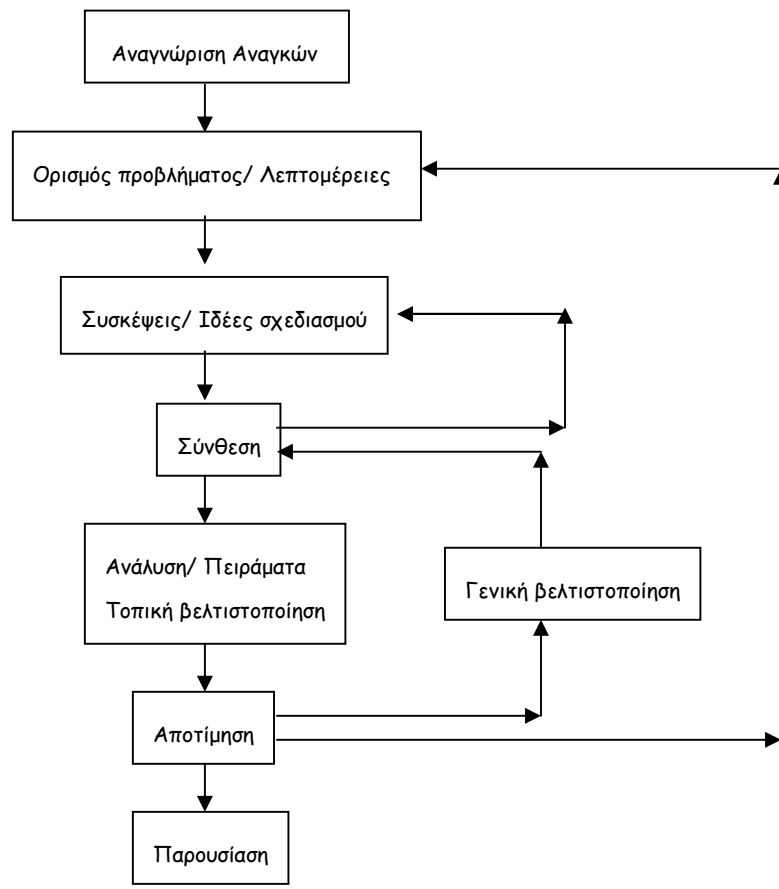
$$\sigma_l = \frac{\sigma_x + \sigma_y}{2} - \left[\frac{(\sigma_x - \sigma_y)^2}{4} + \tau_{xy}^2 \right]^{1/2}$$

$$\phi = \frac{1}{2} \tan^{-1} \left[\frac{2\tau_{xy}}{\sigma_x - \sigma_y} \right]$$



. 1.5:

Mohr



. 1.6: μμ μ .

. 1.1 :

μ

μ

	E-glass/ Epoxy	S-glass/ Epoxy	E-glass/ Isophthalic Polyester	Kevlar 49/ Epoxy	Carbon/ Epoxy AS4/3501-6	Carbon/ Epoxy T800/3900-2	Carbon/ Epoxy IM7/8551-7	Carbon/ PEEK AS4/APC2	Carbon/ Polyamide AS4/Avimid K- III
[g/cm ²]	2.076	1.993	1.85	1.380	1.58	-	-	1.6	-
μ F_1 [GPa]	45	55	37.9	75.8	142	155.8	151	138	110
F_2 [GPa]	12	16	11.3	5.5	10.3	8.89	9.0	10.2	8.3
μ G_{12} [GPa]	5.5	7.6	3.3	2.07	7.2	5.14	5.6	5.7	-
Poisson ν_{12}	0.19	0.28	0.3	0.34	0.27	0.3	0.3	0.3	-
μ F_{1t} [MPa]	1020	1620	903	1380.0	1830	2698	-	2070	-
F_{2t} [MPa]	40	40	40	34.5	57	-	-	86	37
μ F_6 [MPa]	60	60	40	44.1	71	-	-	186	63
μ F_{1c} [MPa]	620	690	357	586.0	1096	1691	-	1360	1000
F_{2c} [MPa]	140	140	68	138.0	228	-	-	-	-
μ (F_4 F_5) [MPa]	60	80	76	48.69	-	-	-	150	-
μ μ ν_{1t} [%]	2.3	2.9	2.4	1.8	1.29	1.68	1.64	1.45	-
μ 6°C] μ . CTE ν_1 [10 ⁻⁶]	3.7	3.5	6.5	-2.0	-0.9	-	-	0.5	-
6°C] μ . CTE ν_2 [10 ⁻⁶]	30	32	22	60	27	-	-	30	-
μ ν_1	0	0	0	0.01	0	0.0095	-	-	-
ν_2	0.2	0.2	0.2	0.2	0.2	0.321	-	-	-
V_f [%]	60	60	50	60	60	-	57.3	61	-
V_v [%]	-	-	2.0	-	-	-	0.1	-	0.5
$\mu\mu$ [deg]	-	-	3.53	-	-	-	-	-	- 10

. 1.2 :

μ

μ μ

E-glass.

μ		μ 0			μ 45		V _f [%]	μ [mm]	g/cm ²
		F _x [MPa]	E _x [MPa]	/ [Nm/g]	F ₄₅ [Mpa]	E ₄₅ [MPa]			
1500	μ	128		89.995	128	6752			
[CSM]		179	7303	125.852	179	7303			
	μ	212	6960	149.054	212	6960			
	μ	24.8		17.437	24.8		17.1	1.041	1.4223
CM1808	μ	201	13780	130.030					
[CSM/0/90]		187	11713	120.973					
	μ	310	13091	200.453					
	μ	20.3		13.132			26.6	1.219	1.5458
TVM 3408	μ	229	15502	139.244	214	14469			
[CSM/+45/0]		262	17914	159.309	250	17914			
	μ	386	16536	234.708	351	15158			
	μ	24.1		14.654	22.7		34.2	1.727	1.6446
XM 2408	μ	98	10680	58.299	236	15158			
[CSM/+45]		228	15158	135.634	262	22392			
	μ	222	10335	132.064	400	16536			
	μ	24.4		14.515	28.8		37.0	1.422	1.6810
UM 1608	μ	214	12746	134.701					
[CSM/0]		228	13091	143.514					
	μ	310	13091	195.128					
	μ	25.5		16.051			29.9	1.143	1.5887

μ μ R-glass μ μ
 (filament winding) sheet molding compounds .
 μ 3,5 GPa μ -glass 4,8 GPa (ASTM D3379) μ
 μ S-glass, μ
 μ glass 2,1 GPa μ S-glass (50% μ , 1,75 GPa -
). μ .
 (μ μ). μ .2.2.
 μ , μ μ
 μ μ μ μ (275 C μ μ
 μ). μ μ μ
 (static fatigue stress corrosion). μ μ μ μ μ μ
 3,5 (μ μ) μ μ μ
 μ 9,5 – 24,77 microns μ μ . μ



(a) μ



(b) 1/4"



(c) 1/32"



(d) 1/16"



(e) E-Glass 7781



(f) E-Glass 120

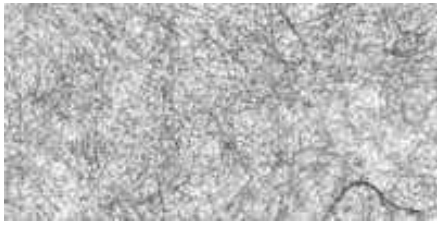


(g) E-Glass μ



(h) E-Glass

... (...)
 ...
 ... (2.1).
 ... polyacrylonitrile (...) pitch (...).
 2.1.
 ...
 2.1, 300, AS2 AS4D
 (IM=Intermediate Modulus), S4 (HS=High Stiffness), 6 ... (HM=High Modulus),
 50 100 (UHM=Ultra High Modulus),
 ...
 ... 50 ... 50%
 ... 1/4 ...
 ...
 ...
 ... 315-537°C,
 ...
 ...
 ... (2,25 3,5) ...
 ... (insulating barrier) ... (...)
 ... 0,5mm)
 O ... HS (\$20/Kg) ...
 ...
 ...
 ...
 ...
 ...
 ...
 ...
 ...



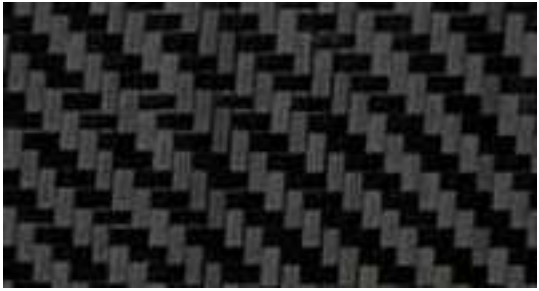
(a) Graphite veil



(b) Weave Graphite Fabric (6K, 5HS)



(c) Plain Weave Graphite Fabric (3K)



(d) Twill Weave Graphite Fabric (3K, 2x2)



(e)



(f)

Technora (aramid), Kevlar, DuPont, Teijin, Akzo Nobel (aramid), Twaron. (aramid), Kevlar 49 (polyethylene) Kevlar49 (UV). 177 C (120 C). 75-80% Kevlar 49



(a) Kevlar veil



(b) Kevlar pulp



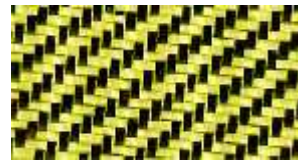
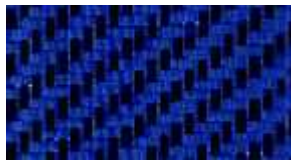
(c) Kevlar fabric



(d) Kevlar tapes



(e) Kevlar/Carbon Hybrid Tapes



(f) Kevlar/Carbon Hybrid Tapes (red, blue, yellow)

μ , μ , μ
 (boron). μ , μ , μ
 μ , μ , μ
 μ μ μ μ μ μ μ μ μ (μ μ μ)
 \$2.000/Kg μ μ μ
 Silicon Carbide (SiC) μ μ μ μ μ μ μ μ μ μ μ μ
 SiC μ μ μ μ μ μ μ μ μ μ μ μ μ
 μ SiC μ μ μ μ μ μ μ μ μ μ μ μ μ
 μ μ μ μ μ μ μ μ μ μ μ μ μ μ μ
 , μ μ μ μ μ μ μ μ μ μ μ μ μ μ μ
 , μ μ μ μ μ μ μ μ μ μ μ μ μ μ μ
 μ μ μ μ μ μ μ μ μ μ μ μ μ μ μ
 μ μ μ μ μ μ μ μ μ μ μ μ μ μ μ
 μ μ μ μ μ μ μ μ μ μ μ μ μ μ μ
 μ μ μ μ μ μ μ μ μ μ μ μ μ μ μ
 μ μ μ μ μ μ μ μ μ μ μ μ μ μ μ μ



Thixotropic Silica

μ μ

end, (Strand, tow, end, yarn roving): strand, tow,
 continuous filaments) (untwisted bundle of
 (furnace) yarn rovings
 yield. yield yield (yd/lb). H
 1000 g/Km. T TEX yield

$$[g/Km] = 496,238/ YIELD[yd/lb] \quad (2.1)$$

(cross-sectional area)
 $[cm^2] = 10^{-5} * [g/Km] / r [g/cm^3]$ (2.2)
 direct-draw roving (spool)
 indirect-draw roving strands yield.
 direct-draw rovings roving
 roving
 fiberglass rovings yields 56 250 yd/lb (8861
 1985 g/km). 3 36 (198 2290).

(mat, fabric veil): To mat
 mat, CSM) (chopped strand mat), swirled filaments (continuous strand
 mat (binder).
 veils mats
 rovings tows (fabric)
 (interloping/ knitting) (woven fabric) (interlacing weaving) yarns. O
 (nonwoven fabrics) strands
 (woven fabrics) (nonwoven fabrics)
 (binder) mat (backing)
 (backing). (chopped strand mats)
 fiberglass) (. .
 backing (nonwoven fabrics),
 . Stitched

nonwoven fabrics μ μ μ (fabrics),
 μ μ μ μ μ (balanced) μ μ μ μ μ
 «off-axis» (. . . \pm , . μ μ +
 -),
 mat, fabric veil μ , μ [gr/m²]
 μ , .2.3. μ



(a) Continuous Strand Veil Surfacing



(b) Chopped Strand Mat (3/4 ounce)



(c) Chopped Strand Mat (1 1/2 ounce)



(d) Continuous Strand Mat



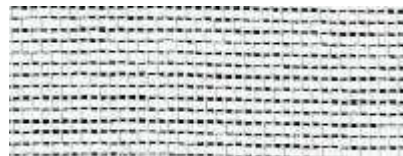
(e) Woven Roving



(f) 2 Oz. Fabric



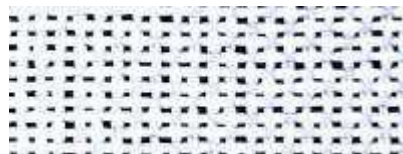
(g) 4 Oz. Fabric: 50 inch wide



(h) 6 Oz. Fabric: 38 inch wide



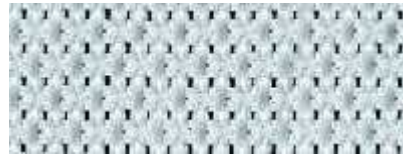
(i) 7 1/2 Oz. Fabric



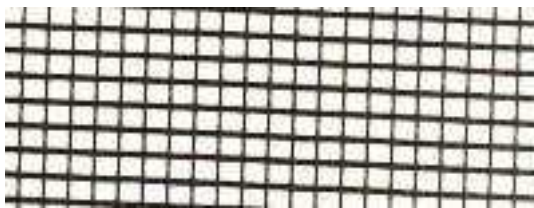
(g) 10 Oz. Fabric



(k) Knit Bi-axial Style 1815 (0/90)



(l) 10 Oz. Fabric



(m) Scrim Fabric, Black



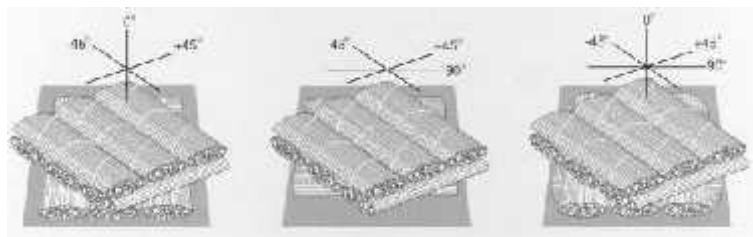
(n) Scrim Fabric, White



(o) Woven Fiberglass Tapes



(p) Gun Roving



(q) Diagram of Stitched Triaxial and Quadraxial Fabrics

2.2

μ μ μ
μ (μ μ) μ ,

2.2.1

(thermoset) matrix (thermoset) resin system (thermoset) thermoset
 (impregnation) thermoset thermoset
 . Shelf life (degradation). Shelf life . Pot life gel
 time gel time
 ASTM D2471 ASTM D3532 carbon-epoxy prepreg.
 (cure) / (gelation)
 D2471). (cure) (probed) (storage life)
 epoxy 8% 4%
 (pigments) UV.
 vinylester, epoxy phenolics. (thermoset) : polyesters,
 (polyesters) (epoxy) (thermoset).

(POLYESTER RESINS):

(unsaturated) (styrene)
 (reactive monomers), (free radical initiator),
 cross-linking (thermoset) (three-dimensional)
 (activators).
 (polyester) vinyl toluene, (styrene)



Polyester Molding

(30) (polyester) UV (styrene) methyl methacrylate (MMA) Styrene-MMA (refractive index) polyester polyesters UV, polyester (filler) (polyester), (halogens) polyester. (chlorendic) bisphenol-A (BPA) fumarate polyester. hydrofluoric . 2.4. "clear castings neat resin samples". (isophthalic) (orthophthalic). BPA fumarate (chlorendic) (isophthalic) 82°C. (peroxides hypochlorites). (isophthalic) (brominated versions) . 2.4. (orthophthalic), (polyesters) (chlorentic) 176°C. (peroxides hypochlorites).

BPA fumarate (isophthalic) 121°C. (peroxides hypochlorites).
 (polyesters) 1,43 \$/Kg (2,22 \$/Kg).

VINYLESTER: (polyesters) vinyl ester (epoxy) 121°C. (peroxides hypochlorites). (brominated versions) 2.4. (polyesters) (epoxy), 4,0 \$/Kg.



Vinyl-Ester

(EPOXY): (epoxy) (adhesives). (aircraft honeycomb) (tooling). 5° 150°C. (epoxy) (adhesives)



2000 Epoxy

(casting compounds) ,
 ,
 potting
 (impregnating) (epoxy)
 vinyl ester.
 ()
 2.4. 9310/9360 33 phr (phr= parts per hundred in
 weight= 9310 9360.
 9420/9470 (filament
 Resin Transfer Molding (RTM= (pultrusion) (prepregs).
 winding), 9420 () 24,4 phr () 32,4 phr
 9470. 2.4. T_g
 (glass transition temperature) « »
 (service) 125°C 175°C.
 (thermoset), (thermoplastics).
 epoxies (247°C) (toughened epoxies) (brittle
 185°C) 76

(PHENOLIC):

Sheet Molded Compound
 (SMC), (filament winding) (pultrusion).
 (phenolic) (polyester)
 (thermoset), (polyester)
 (polyester) \$1,32/Kg.
 (toxicity) bismaleimide polystyrylpyridine.
 bismaleimide, 70/30 compimide
 796 TM-123 Shell Chemical Co. 2.4.

2.2.2 (thermoplastic)

(thermoplastic) ,
 ,
 .

(thermoplastic)

(thermoplastic)

10 100

(thermoplastic)

(viscous effects)

(impregnation)

polymer strand

(intermingled)

(thermoplastic)

(thermoplastic)

(softened)

stage) Poly-ether ether-ketone (PEEK)

(thermoplastic)

(0,5% epoxies)

polyphenylene sulfide (PPS)

(thermoplastic)

polysulfone (PSUL)

polyetherimide (PEI) polyamide-imide (PAI)

T_g

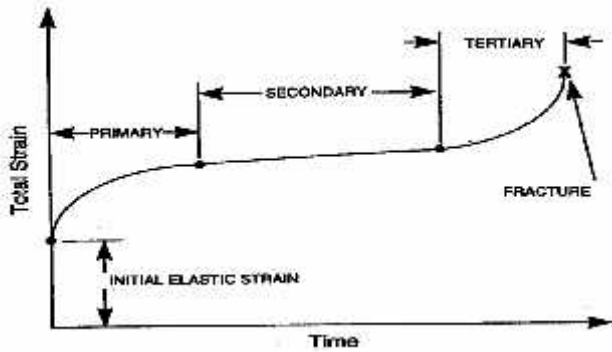
LARC-TPI, (prepolymers)

300°C

(thermoplastic)

(solvent solution)

(coatings)



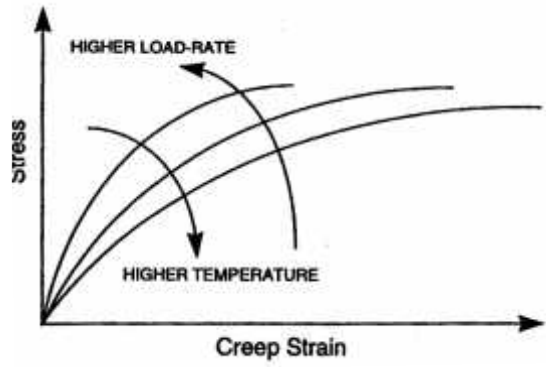
. 2.1:

2.2.3

(viscoelastic)

(=)

(. 2.1).



2.3:

T_{gc} , T_g , T_{gd}

 PMCs.

$$T_{gw} = (1 - 0,1m + 0,005m^2) T_{gd} \quad (2.4.)$$

T_g ($d=dry$), T_{gw} , T_{gd}

 m

 retention ratio (g)

$$g = [(T_{gw} -) / (T_{gd} -)]^{0,5} \quad (2.5)$$

Analysis DSC=Differential Scanning Calorimetry, DTA=Differential Thermal

 E1356. ASTM D3418

 PMCs

 (HDT= Heat Deflection Temperature),

 (Heat Distortion Temperature)

 D648. 1,82 MPa 0,455 MPa

 point bending) (deflection)

 0,25mm. H HDT.

 DSC (polymer), HDT T_g

2.2.4

(degradation) PMC UV

« »

PMC

Barcol (ASTM D2583).
(acetone)

DSC=Differential Scanning Calorimetry,
DSC (sweep)

DSC

H_R (heat of reaction)
(post-cure). DSC
(total heat of reaction) (ASTM
($0 < < 1$))

D3418 D5028).
 $= 1 - H_R /$

FRP (ASTM C581) (barrier)

2.2.5

(polymers)
 ASTM 84 PMCs
 (forced air tunnel),
 (FSC=Flame Spread Classification),
 0 FSC 25, 100 FSC, 25<FSC 75, FSC>75.
 (ASTM D2863) ASTM 906
 (radiant heat). ASTM 162. ASTM 662.
 98°C, (isophthalic) (vinylesters) 135°C, fumarate
 (chlorendic) 140°C. (fiber reinforced composites)
 PMCs

. 2.1.

μ

Fiber	Modulus [GPa]	Tensile Strength [GPa]	Compression Strength [GPa]	Elongation [%]	Density [gr/cc]	Longitudinal Thermal Expansion [10 ⁻⁶ / C]	Transverse Thermal Expansion [10 ⁻⁶ / C]	Poisson Ratio	Thermal Conductivity [W/m/ C]	Maximum Operating Temperature [°C]	Resistivity [microhm-m]
	[GPa]	[GPa]	[GPa]	μ [%]	[gr/cc]	μ [10 ⁻⁶ / C]	μ [10 ⁻⁶ / C]	Poisson	μ [W/m/ C]	M μ [°C]	[microhm-m]
E-Glass	72.345	3.45	-	4.4	2.5-2.59	5.04-5.4	-	0.22	1.05	550	-
S-Glass	85	4.8	-	5.3	2.46-2.49	1.6-2.9	-	0.22	1.05	650	-
C-Glass	69	3.31	-	4.8	2.56	6.3	-	-	1.05	600	-
D-Glass	55	2.5	-	4.7	2.14	3.06	-	-	-	477	-
Carbn											
T300	230	3.53	-	1.5	1.75	-0.6	7-12	0.2	3.06	-	18
M50	490	2.45	-	0.5	1.91	-	-	-	54.43	-	8
AS2	227	2.756	-	1.3	1.8	-	-	-	8.1-9.3	-	15-18
AS4-D	241	4.134	-	1.6	1.77	-0.9	-	-	8.1-9.3	-	15-18
IM6	275.6	5.133	-	1.73	1.74	-	-	-	8.1-9.3	-	15-18
HMS4	317	2.343	-	0.8	1.8	-	-	-	64-70	-	9-10
UHM	441	3.445	-	0.8	1.85	-	-	-	6.5	-	120
P55	379	1.9	-	0.5	2	-1.3	-	-	120	-	8.5
P100	758	2.41	-	0.32	2.16	-1.45	-	-	520	-	2.5
Kevlar 29	62	3.792	-	-	1.44	-	-	-	-	-	-
Kevlar 49	131	3.62	0.72	2.8	1.45	-2	59	0.35	0.04	160	-
Kevlar 149	179	3.62	0.69	1.9	1.47	-	-	-	-	-	-
Technora	70	3	0.6	4.4	1.39	-6	59	0.35	-	160	-
Boron	400	2.7-3.7	6.9	0.79	2.57	4.5	0.2	0.2	38	315	-
SCS-6	427	2.4-4	-	0.6	3	4-4.8	-	0.2	10	-	-
Nextel	260	2.1	-	-	3.4	6	-	-	-	1200	-

. 2.2 : μ μ .

Fiber/	Strength reduction / (%)
E-glass	25-50
S-2 glass	24
Kevlar 49	31
Kevlar 149	14
Carbon ASW-4	17
Carbon T-700	22
Carbon IM-6	21
Carbon T-40	21

. 2.3 : (stitched fabrics).

Denomination / μ	Chopped Strand Mat g/m^2	0/90 (balanced) g/m^2	± 45 (balanced) g/m^2	0 (warp) g/m^2	90 (weft) g/m^2
M1500	450	-	-	-	-
C24	-	800	-	-	-
CM1808	225	600	-	-	-
CM1810	300	600	-	-	-
Q30	-	-	440	405	170
QM5620	600	1100	800	-	-
TH27	-	-	450	-	450
TVM3408	225	-	609	541	-
UM1810	300	-	-	600	-
UM1608	240	-	-	533	-
XM2408	225	-	800	-	-

. 2.4 :

μ μ

-“thermoset”.

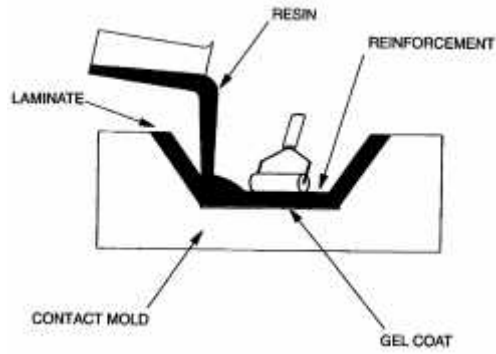
Thermosets	Tensile Modulus [G a]	Tensile Strength [MPa]	Compression Strength [MPa]	Shear Strength [MPa]	Tensile Elongation [%]	Flexural Modulus [G a]	Flexural Strength [G a]	Thermal Expansion [10 ⁻⁶ / C]	Heat Deflection Temperature [C]	Poisson Ratio	T _g [C]	Density [gr/cc]
μ μ	[G a]	[MPa]	[MPa]	[MPa]	μ [%]	μ [G a]	μ [G a]	μ [10 ⁻⁶ / C]	μ H.D.T. [C]	Poisson	T _g [C]	[gr/cc]
POLYESTER												
Orthophthalic	3.4	55.2	-	-	2.1	6.9	220.7	-	79.4	0.38	-	-
Isophthalic	3.4	75.9	117.2	75.9	3.3	7.6	241.4	30	90.6	0.38	-	-
BPA Fumarate	2.8	41.4	103.5	-	1.4	9	158.6	-	129.4	0.38	-	-
Chlorendic	3.4	20.7	103.5	-	-	9.7	193.1	-	140.6	0.38	-	
VINYL ESTER												
Derakane 411-45	3.4	82.7	117.1	82.7	5-6	3.1	124	-	104	0.38	-	-
EPOXY												
9310/9360@23 C	3.12	75.8	-	-	4	-	-	54	-	0.38	185	1.2
9310/9360@149 C	1.4	26.2	-	-	5.2	-	-	-	-	-	185	1.2
9420/9470(A)@23 C	2.66	57.2	-	-	3.1	-	-	-	-	-	195	1.162
9420/9470(B)@23 C	2.83	77.2	-	-	5.2	-	-	-	-	-	155	1.158
HPT1072/1062-M@23 C	3.383	-	-	-	-	3.383	131	-	-	-	239	-
BISMALEIMIDE												
796/TM-123@24 C	3.582	-	-	-	-	3.582	132	-	-	-	260	33
796/TM-123@249 C	-	-	-	-	-	2.48	90	-	-	-	260	-

. 2.5 :

μ

- “thermoplastic”.

Thermoplastics	Tensile modulus [GPa]	Tensile Strength [MPa]	Tensile Elongation [%]	Poisson Ratio	Thermal Expansion [10 ⁻⁶ / C]	T _g [C]	T _m [C]	Process Temperature [C]	Heat Deflection Temperature [C]	Fracture Toughness G _{IC} [KJ/m ²]	Density [gr/cc]
μ	- [GPa]	[MPa]	μ [%]	Poisson	μ [10 ⁻⁶ / C]	T _g [C]	T _m [C]	μ [C]	H.D.T. [C]	G _{IC} [KJ/m ²]	[gr/cc]
PEEK	3.24	100	50	0.4	47	143	343	400	160	4.03	1.32
PPS	3.3	82.7	5	0.37	49	90	290	343	135	-	1.36
PSUL	2.48	70.3	75	0.37	56	190	-	300	174	2.45	1.24
PEI	3	105	60	0.37	56	217	-	343	200	2.8	1.27
PAI	2.756	89.57	30	0.37	36	243	-	300	274	3.5	1.4
K-III	3.76	102	14	0.365	-	250	-	-	-	1.9	1.31
LARC-TPI	3.72	119.2	5	0.36	35	264	325	343	-	1	1.37



. 3.1:

()
 , , ,
 ,
 (release agent)
 alcohol), (silicones) (wax), (poly-vinyl
 (release papers).
 (mineral-filled) (pigmented)
 (chopped strand mat), (cloth),
 (woven roving).
 . 3.1

. 3.2.

(hand lay-up)
 (tooling) (runs)
 \$20/ Kg

bagging (thermosets) (thermoplastics) *bagging*
 370 C. *Kapton vacaloy* (thermoplastics)
 260-370 C (thermosets). 120-180 C (thermoplastics)
 (good flow compaction). (thermoplastics)
 (thermoplastics)
 (thermoplastics)
 ,
 μ (

3.4 -«autoclave processing»

O (autoclaves)
 (vacuum) (vacuum bag).
 (vacuum bag)
 (cure)
 (autoclaves)
 (domed ends),
 1m,
 1 8m.
 (tools for autoclaves)
 (bag).
 (cast epoxy tooling)

()

(*bagging*).

,

,

,

3-5 12 16

3.5 – compression molding

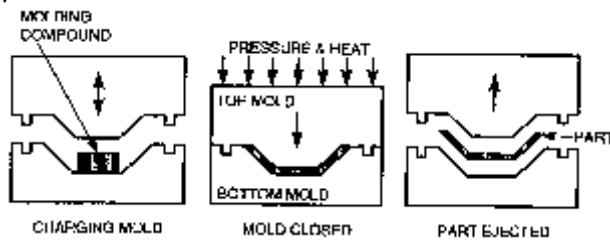
(*compression molding*)

(*compression molding*)

(15 24)

100 4.000t 1 kgr 75 kgr.

(*compression molding*),



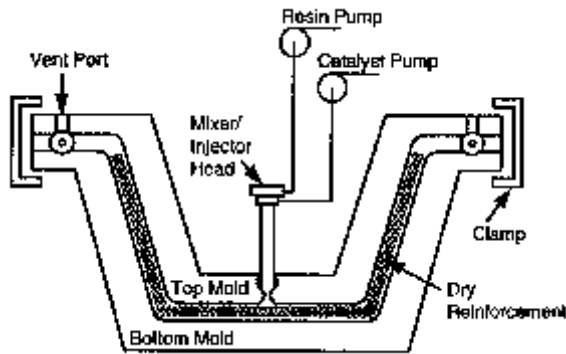
. 3.3:

(Sheet Molding Compound).
 BMC (Bulk Molding Compound) 20-50%.
 150 200 C
 SMC (Sheet Molding Compound) BMC (Bulk Molding Compound).
 150 200 C
 BMC (Bulk Molding Compound) SMC (Sheet Molding Compound) fiber preforms prepreps.
 3-4 7-14

3.6 - resin transfer molding (rtm)

- Resin Transfer Molding (RTM)
 Resin Transfer Molding (RTM)

Resin Transfer Molding (RTM).



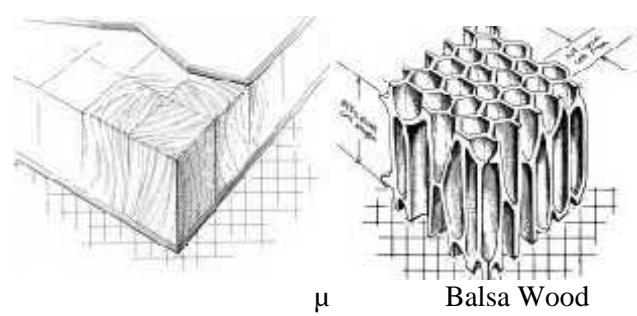
. 3.4:

Vacuum Assisted Resin Injection Molding (VARIM)

(vacuum bag).
 SCRIMP.
 RTM, RTM

preform molding (open tooling) preform
 preform.
 preform screen) (binder), (perforated
 (corresponding bonding agent) 75%
 Structural Reaction Injection Molding (SRIM) preform
 Flexible Resin Transfer Molding (FRTM),
 Resin Transfer Molding (RTM)
 contoured mold Resin Transfer Molding (RTM)
 preform () Resin Transfer Molding
 (RTM) (scrap losses)
 Resin Transfer Molding (RTM).
 12mm. H Resin Transfer Molding (RTM),
 ± 0,2mm.
 (Resin Transfer).

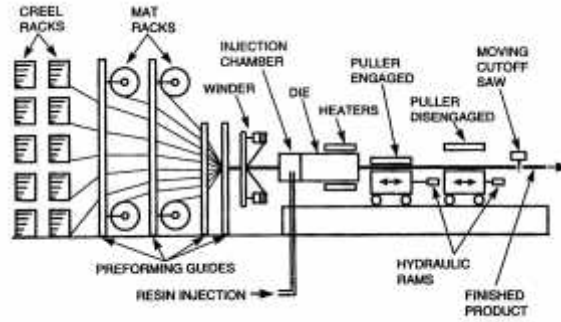
RTM
 RTM 45Kg/min
 2-8 /
 (spray-up).
 3,65m 3,0m
 272Kg
 3,8cm 45,7cm.



RTM ()
 RTM (vacuum bag) 1/3
 prepreg, prepreg,
 prepreg, 80%
 lay-up), RTM (hand
 (equipment depreciation),
 (scrap rate)
 RTM (hand lay-up).
 SMC injection molding.

3.7 - pultrusion

(pultrusion)
 performing guides
 (cross-section)
 (cross-section)
 (injection chamber),
 (injection chamber)
 (reciprocating pullers),
 (moving cut off saw)



. 3.4:

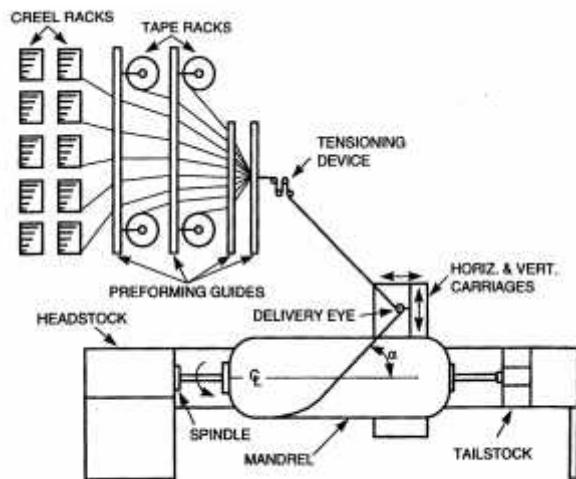
(reciprocating pullers) (caterpillar puller) (friction). (resin bath) (injection chamber) (associated pressurization tank). (VOC=VOLatile Content) (styrene) 1% (pultrusion) (injection chamber), (rotating winder) (drive shafts). (fiber preheaters) (thermoplastic) (radio-frequency [RF] heaters), (thermoplastic) prepregs prepregs (pultrusion) (polyesters, vinyl-esters, epoxy, phenolics). (thermoplastics) (polyesters, vinyl-esters) (roving continuous strand mat [CSM]), stitched bidirectional materials. (thermoplastics)

(pultrusion) (roving longitudinal fibers) (stitched) (fillers) 45%, 30%
 (pultrusion) (fillers) 12mm standard conduction heaters (interlaminar cracking).
 tunnel-oven, (roving mat) tunnel-oven downstream (resin bath) sizing brush, (pultruded part) tunnel-oven tunnel-oven tunnel-oven.
 (cross-section) pulforming, step-molding pulforming, (roving mat) (impregnating bath). leaf
 20m²/min. 2m/min,

3.8 - filament winding

(filament winding), (mandrel) (roving) (delivery eye) (helical winding machine).

(polar). (lathe).
 5 -90 , hoop winding. (carriage).
 (2ply balanced laminate)
 (resin bath)
 (complicated contours). (helical winder)
 (yaw) (winders)
 (geodesic path), (helical winder),
 (winder),
 (set) (slip string)
 (resultant) hoop meridional forces,
 (dome).



. 3.4:

(polar winders),
 ,
 ,

(planar path).
 (polar winding)
 $(r_2 < 0)$,
 (revolution).
 (soluble sand mandrel)
 polyvinyl alcohol. To
 (low runs)
 (wet re-rolled) preregs
 (slippage)
 (vacuum) (autoclave)
 (set up removal)
 0,6-1,2m/sec
 (wet fiber set up).

3.9

Polymers), (Fiber Reinforced Polymers),

80 C.

3.4 :

	$Kg/m^3 \times 10^3$	(GPa)	Poisson	(MPa)	μ (%)
	1,90	380	0,35	2100	0,6
f_i	1,80	230	0,35	2700	1,3
E	2,54	72-75	0,25	3500	4,8
Z (AR)	2,27	70-76	0,25	2500-3500	3-4,6
S2	2,44	85-88	0,25	4600	5
μ					
Kevlar 29	1,45	65	0,32	3500	4
Kevlar 49	1,44	125	0,32	3500	2,1
	7,86	200	0,28	400-1700	10

3.5 :

	(GFRP)	(GPa)	μ (%)
μ	50		3
μ	65-120		2-3
μ	35-190		1-1,5
	200		10

4.

4.1

The text in this section is extremely faint and illegible, appearing to be a series of characters and symbols that do not form recognizable text.

Boltzmann (1876),

$$\sigma(t) = \int_{-\infty}^t G(t-\tau) d\varepsilon(\tau), \quad (1)$$

The text following equation (1) is extremely faint and illegible.

$$\sigma(t) = \int_{-\infty}^t G(t-\tau) \frac{\partial \varepsilon(\tau)}{\partial \tau} d\tau. \quad (2)$$

The text following equation (2) is extremely faint and illegible.

$$\sigma(t) = \int_{-\infty}^t (E_0 + cg(t-\tau)) \frac{\partial \varepsilon(\tau)}{\partial \tau} d\tau,$$

The text following equation (3) is extremely faint and illegible.

$$\int_0^{\infty} g(t) dt = 1. \quad (3)$$

The text following equation (3) is extremely faint and illegible.

$$\bar{\sigma}(\omega) = E^*(\omega)\bar{\epsilon}(\omega),$$

$$\tilde{\epsilon}(\omega)$$

$$E^*(\omega) = E_0 + i\omega c \tilde{g}(\omega) \quad (4),$$

$$E^*(\omega) = E'(\omega) + iE''(\omega),$$

$$\eta(\omega) = \frac{E''(\omega)}{E'(\omega)}$$

(Ward and Hadley (1993), Park (2001)),

Adhikari (2000)

Park (2001)

σ_∞

$g(t)$

$$\sigma_0 = E_0 \epsilon_0$$

(Crawford, 1998),

t_0
 $g(t)$

1

1.

(t),

1.

(Ward and Hadley (1993))

Table 1
Exponential and hyperbolic models in time and frequency domains

	Exponential	Hyperbolic
$\sigma(t)$	$\sigma_0 + (\sigma_\infty - \sigma_0)(1 - \exp(-t/t_0))$	$(\sigma_0 - \sigma_\infty) \frac{t_0}{t_0 + t} + \sigma_\infty$
$g(t)$	$\frac{1}{t_0} \exp(-t/t_0)$	$\frac{t_0}{(t_0 + t)^2}$
$\tilde{g}(\omega), \omega \geq 0$	$\frac{1}{1 + i\omega t_0}$	$-\pi\omega t_0 \exp(i\omega t_0)$
$E^*(\omega)$	$E_0 + \frac{c}{t_0} \frac{i\omega t_0}{1 + i\omega t_0}$	$E_0 - i\pi \frac{c}{t_0} (\omega t_0)^2 \exp(i\omega t_0)$

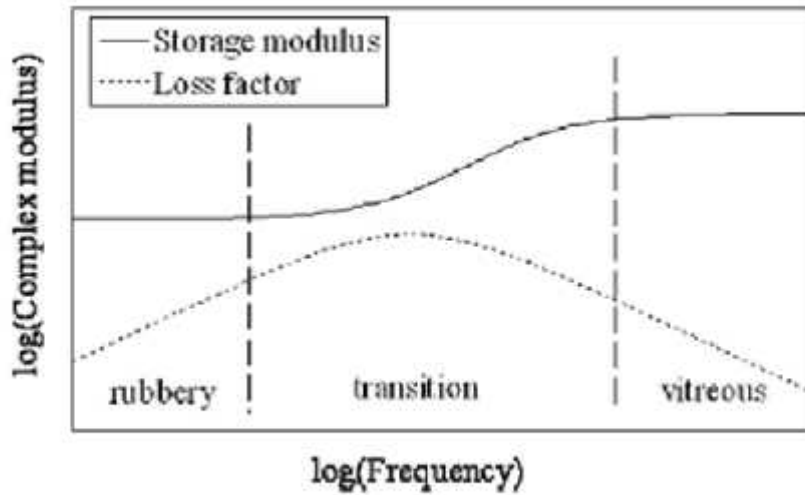


Fig. 1. Complex modulus for exponential model.

Castillo). (Bagley Torvik, 1983 Pritz, 1996, 2003). (Corte

$$\sigma(t) = \sigma_0 + (\sigma_\infty - \sigma_0) \frac{2}{\pi} \arctan\left(\frac{t}{t_0}\right). \quad (5)$$

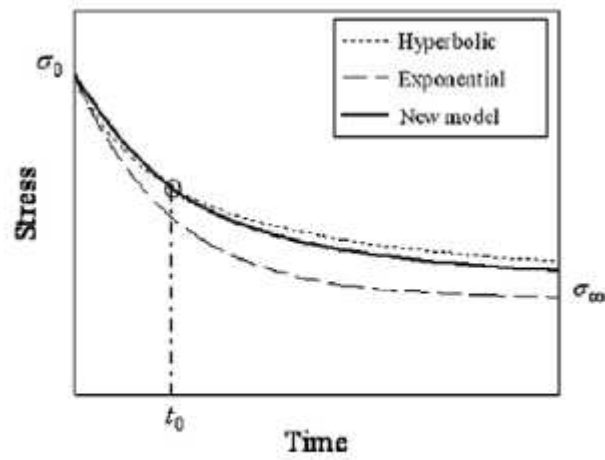


Fig. 2. Stress relaxation under constant strain.

$$g(t) = \frac{2}{\pi} \frac{t_0}{t_0^2 + t^2} \quad (3)$$

$$\tilde{g}(\omega) = 2 \exp(-\omega t_0).$$

$$E^*(\omega) = E_0 + i2 \frac{c}{t_0} \omega t_0 \exp(-\omega t_0), \quad (4)$$

$$E^*(\omega) = E_0 + i2 \frac{c}{t_0} \omega t_0 \exp(-\omega t_0), \quad (6)$$

() = ,

$$K_s = \eta_s^2, \quad (2)$$

3. 4, 10%

Table 2
Storage modulus E and loss factor η for polymer concrete specimens

f (Hz)	E (10^9 Pa)	η
24.9	36.9	0.0106
40.4	38.2	0.0221
85.5	38.0	0.0153
137	38.0	0.0079

Table 3
Parameters for the fitted model

E_0 (10^9 Pa)	ω_0 (rad/s-Hz)	η_0	ζ_0 (10^{-3} s)	c (10^6 Pa s)
38.2	259-41.3	0.0221	3.85	4.42

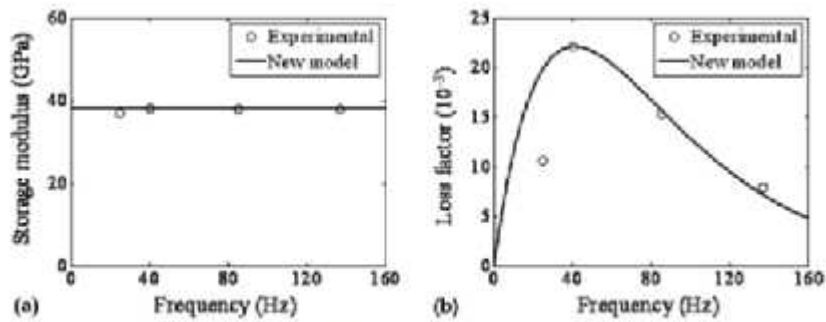


Fig. 4. Comparison between experimental data and fitted model: (a) storage modulus and (b) loss factor.

➤

4.2 GFRP (FRPs)

The GFRP (FRPs) are characterized by their mechanical properties, which are significantly different from those of traditional materials. The GFRP (FRPs) are characterized by their mechanical properties, which are significantly different from those of traditional materials. The GFRP (FRPs) are characterized by their mechanical properties, which are significantly different from those of traditional materials.

The GFRP (FRPs) are characterized by their mechanical properties, which are significantly different from those of traditional materials. The GFRP (FRPs) are characterized by their mechanical properties, which are significantly different from those of traditional materials.

$$\varepsilon_{1,top} = \frac{du_{1,top}}{dx}$$

$$\varepsilon_{1,top} = \frac{du_{1,top}}{dx} \cong \frac{du_{1,a}}{dx} \quad (1)$$

The GFRP (FRPs) are characterized by their mechanical properties, which are significantly different from those of traditional materials. The GFRP (FRPs) are characterized by their mechanical properties, which are significantly different from those of traditional materials.

$$\varepsilon_{1,top} = \frac{t_m}{G_m} \frac{d\tau_a}{dx} \quad (2)$$

$$\tau_a(x) = \frac{P}{b_1} \cdot \beta \cdot \frac{\cosh(\beta x)}{\sinh(\beta L)} \quad (2)$$

The GFRP (FRPs) are characterized by their mechanical properties, which are significantly different from those of traditional materials. The GFRP (FRPs) are characterized by their mechanical properties, which are significantly different from those of traditional materials.

$$\varepsilon_{1,top} = \frac{t_m}{G_m} \cdot \frac{P}{b_1} \cdot \beta^2 \cdot \frac{\sinh(\beta x)}{\sinh(\beta L)}$$

$$\varepsilon_{1,top}(L) = \frac{t_m}{G_m} \cdot \frac{P}{b_1} \cdot \beta^2 \quad (3)$$

$$\beta^2 = \frac{3 \cdot G_1 \cdot G_m}{E_1 t_1 (3 \cdot G_1 \cdot t_m + t_1 \cdot G_m)} \quad (4)$$

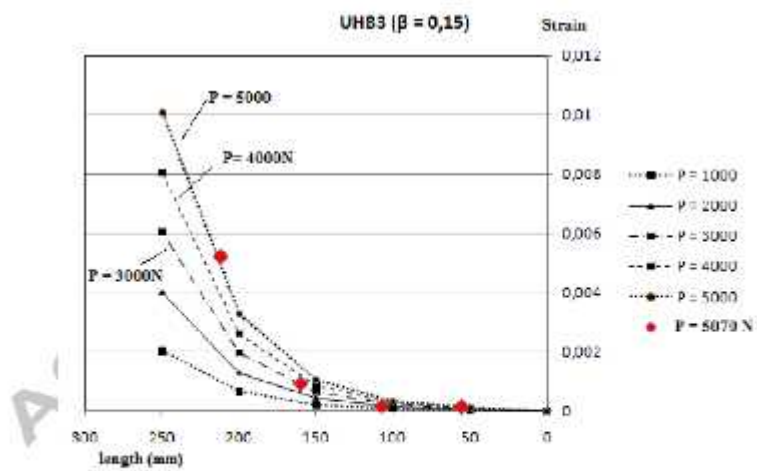
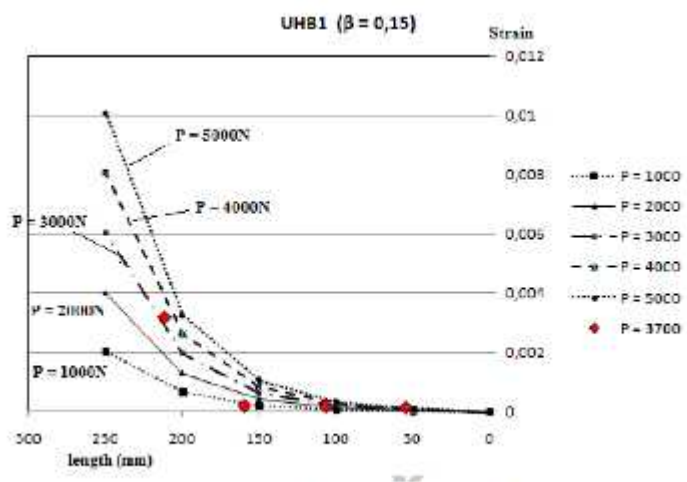
$G_m \nu_1 = 0.22, \nu_m = 0.30$ $E_m = 1760 \text{ N/mm}^2$ $G_1 = \frac{E_1}{2 \cdot (1 + \nu_1)}$
 $t_m = 1.5 \text{ mm} - 3.0 \text{ mm}$ $\nu = 0.053 - 0.026$ $t_m = 1.5 \text{ mm}$
 3.0 mm 3μ μ

$$\varepsilon_{1,top}(L) \approx 7.8 \cdot 10^{-3}$$

$$P = 3350 \text{ N},$$

GFRP.

$$= 0,15.$$



(a)
(b)
Figure 15 – Comparison of theoretical diagrams strain values vs. length of anchorage with experimental values at (a) P=3700N (UH81) and (b) P=5079N (UH83).

μ μ
μ μ μ μ μ μ μ μ μ μ
μ μ μ μ μ μ μ μ μ μ :
μ μ μ μ μ μ μ μ μ μ :
1. μ GFRP μ μ μ
μ μ μ μ μ μ μ μ μ μ
2. μ μ μ μ μ μ μ μ μ μ
3. μ μ μ μ μ μ μ μ μ μ μ μ
4. μ μ μ μ μ μ μ μ μ μ μ μ μ μ
μ μ μ μ μ μ μ μ μ μ μ μ μ μ

4.4 μ : μ

WISPERX, Rayleigh, Palmgren-Miner, Broutman, Sahu, WISPER, Broutman, Sahu.

$$\text{Model Error} - M_e - \log \left(\frac{N_{\text{model}}}{N_{\text{experiment}}} \right)$$

$\epsilon=0$ 1/10 $\epsilon=-1$ 4 11 $-0,3 < \epsilon < 0,7$ DD16 (6), Y1 OH (), PM BF, RS5 BS Y1 INT 117% 192% 26% WISPERX

8, VT8084, RAY95, BF, R, BS, RS1, INT, PM, RS3, RS5, Y1, RS2, RS4, RAY95R01, Y1, RS1, 0,04, VT8084, -0,03, RS1

Table 8
Comparison of model predictions for mean fatigue life under spectrum loading of VT8084 material

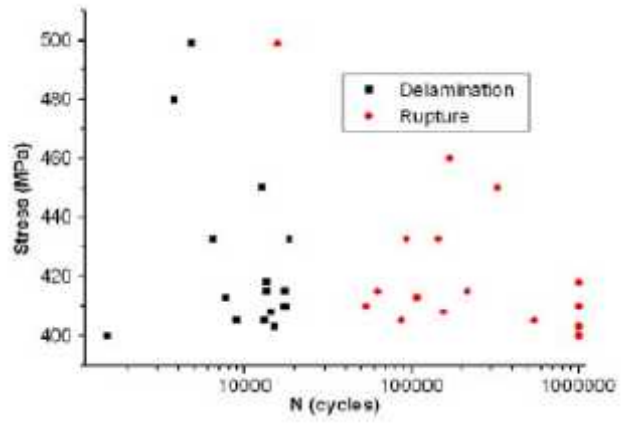
Material	VT8084	VT8084	VT8084
Spectrum	RAY95	RAY95	RAY95R01
max(σ) (MPa)	127.2	107.7	183.8
# Replicates	10	10	5
Average exp. N	265,000	915,000	150,000
# Spectrum repeats	53.1	183	30.1
Model	M_4		
PM	0.00	0.06	0.27
OH	-	-	-
RF	1.85	1.02	0.24
HR	-0.01	0.05	0.27
BS	-0.07	0.04	0.17
RS1	-0.03	0.04	-0.01
RS2	-0.22	-0.23	-
RS3	0.00	0.06	0.17
RS4	-0.19	-0.11	-
RS5	0.00	0.06	0.20
Y1	-0.12	-0.05	-0.32
INT	-0.06	0.02	0.17

9), (VT8084 RAY95) Bond Farrow

Table 9
Comparison of model predictions statistics compiled for all data sets and spectrum loads

Model	max(M_4)	min(M_4)	mean(M_4)	median(M_4)
PM	0.60	0.00	0.24	0.24
OH ^a	0.37	-0.20	0.08	0.07
RF	1.92	0.00	0.65	0.44
HR	0.60	-0.01	0.23	0.24
BS	0.50	-0.09	0.16	0.16
RS1	0.60	-0.03	0.22	0.17
RS2 ^b	0.47	-0.23	0.07	-0.04
RS3	0.50	0.00	0.19	0.17
RS4 ^b	0.48	-0.19	0.13	0.06
RS5	0.55	0.00	0.21	0.19
Y1	-0.03	-0.78	-0.33	-0.31
INT	0.53	-0.06	0.18	0.17

PM, 4



NC2/RTM6

72-60% S*N
 499 400 MPa
 420
 400

Table 1. Weibull parameters of specimen IR.384 A

Stress (MPa)	%UTS	Cycles (N)	Shape Parameter, β	Scale Parameter, α (N), 63,2%
		110639		
410	57	216389	0,86	2.082.204
		575016		
		1593		
482	67	5676	0,82	41.425
		8933		
518	72	2410	0,63	101.653

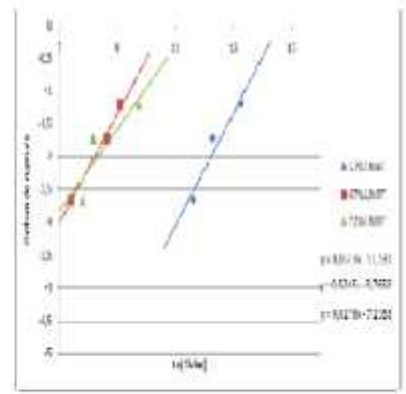


Fig. 4. Weibull parameters Curve - different tension

burn-in,
 1,

Boerstra, $f = Ac^{-p}$ (a^{-m}N), Harris. H

CLD $f = A_1 \log N + B_1$
 $u = A_2 \log N + B_2$
 $v = A_3 \log N + B_3$

CLD μ

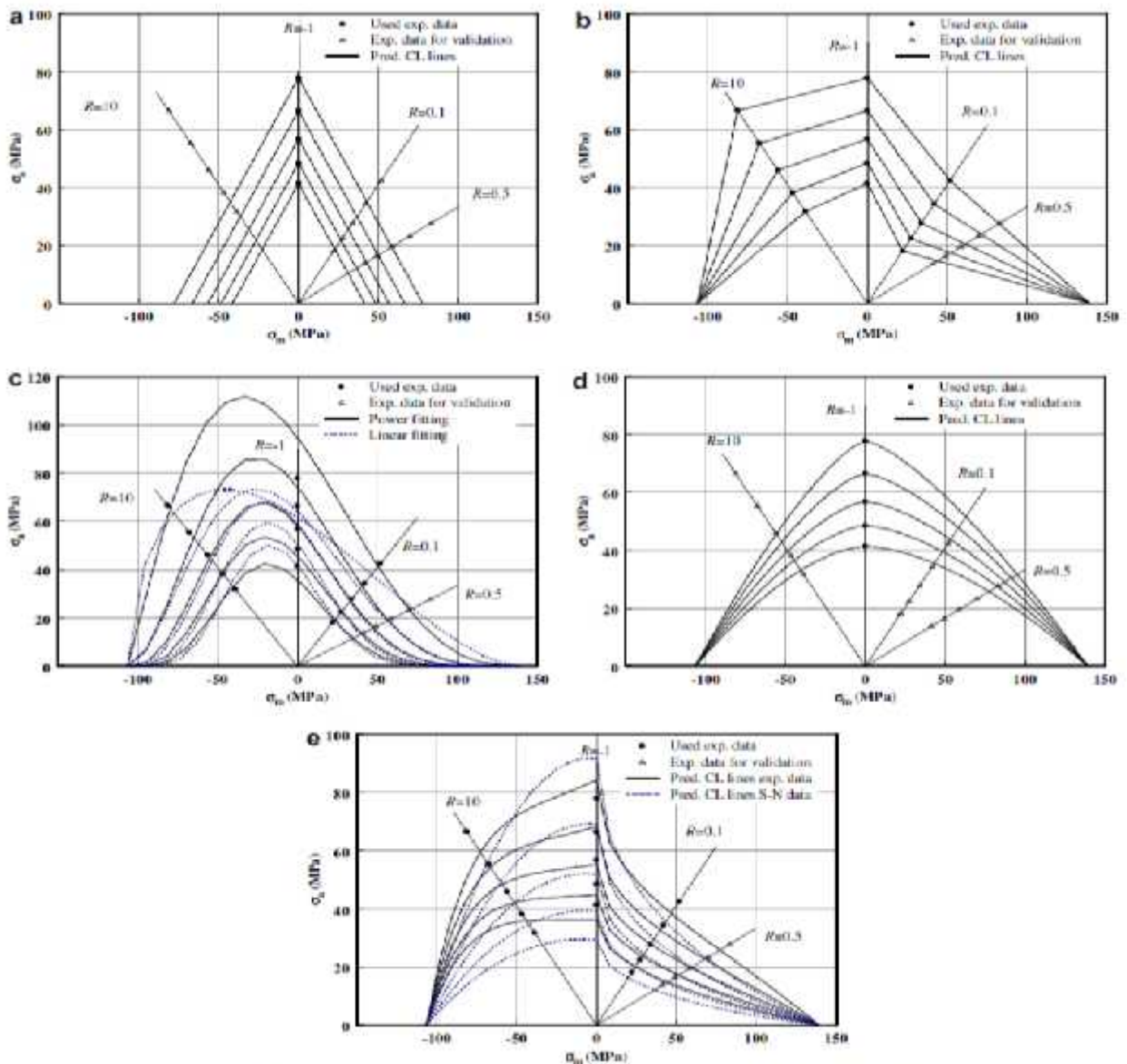
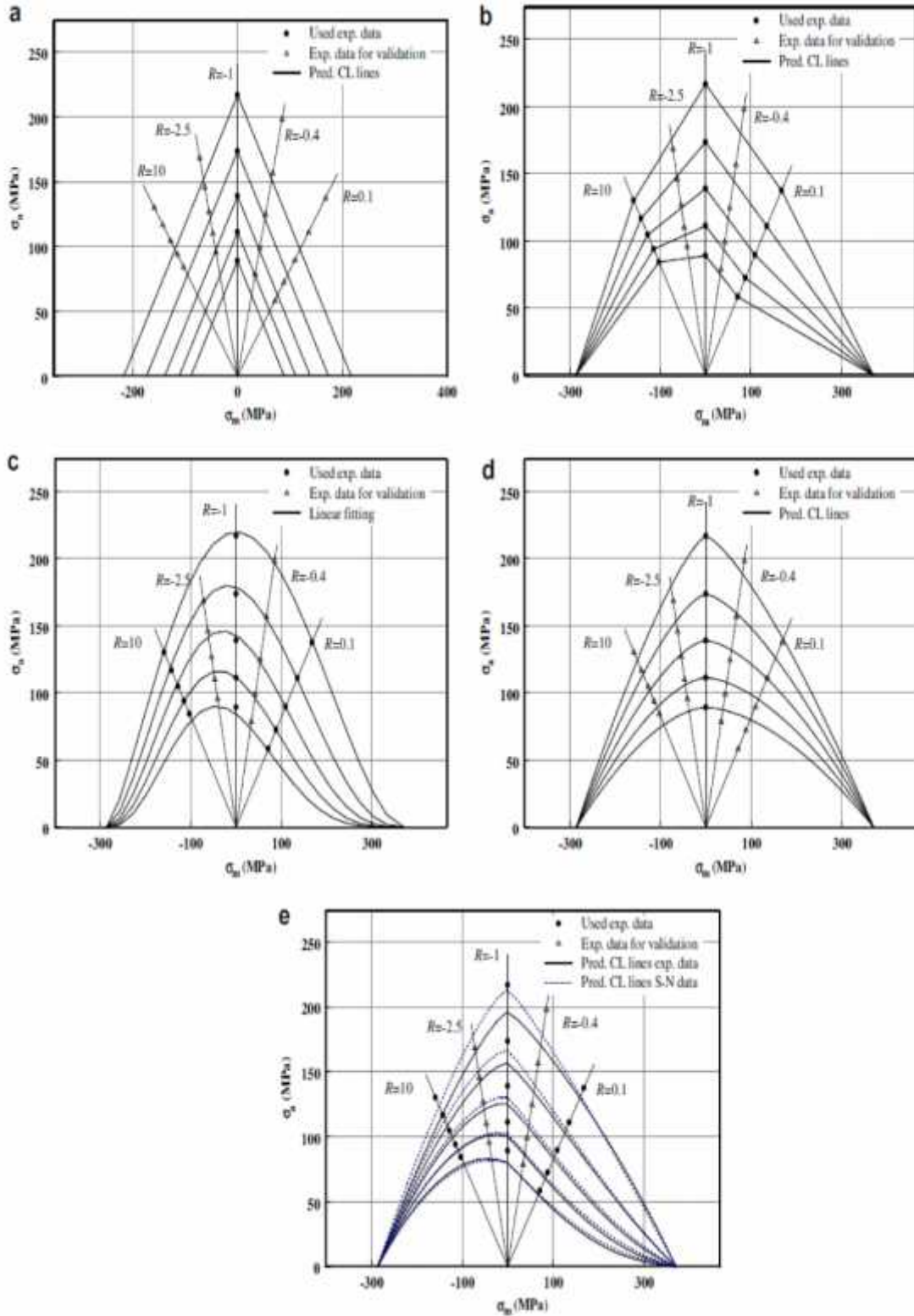


Fig. 2. Constant life diagrams for $N = 10^7 - 10^8$, material #1 (linear-a, piecewise linear-b, Harris-c, Kawai-d, Boerstra-e).

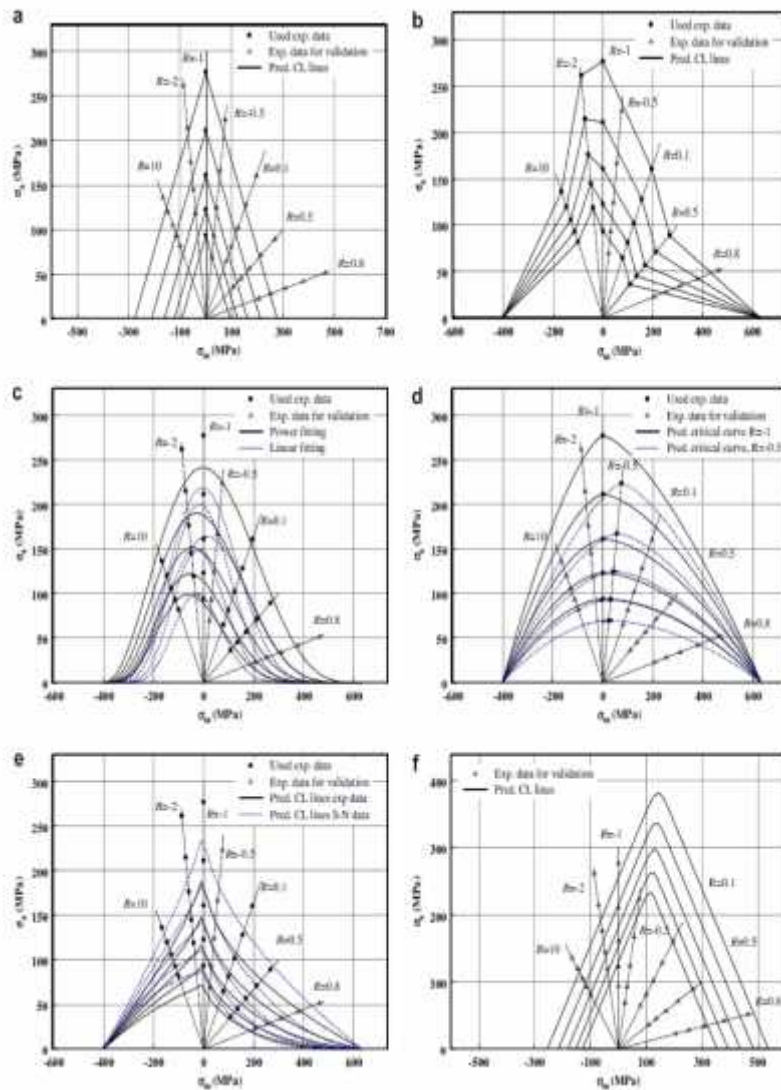
CLD Kawai CLD $R=0,5$ ($R^2 = 0,89$).

S- Kawai.

μ μ CLD μ μ μ , Harris μ μ f μ μ μ μ μ μ μ , Boerstra μ μ S- μ CLD μ



❖ #2
 #1, $R = -1$ S-
Kawai.
 $R = -0.77$, $R = -1$
 Harris
 $f = A_1 \log N + B_1$
 $u = A_2 \log N + B_2$
 $v = A_3 \log N + B_3$
 log-log S-
 3. CLD,
 $R = -0.4$ $R = -2.5$.
Boerstra.



❖ #3
 S- CLD, Kawai
 S- DD16,
 Kawai -0,63, S- R=-0.5
 CFL Kawai.
 Harris
 $f = Ac^{-P}$

$$f = A_1 \log N + B_1$$

$$u = A_2 \log N + B_2$$

$$v = A_3 \log N + B_3$$

S- CLD
Boerstra
 R = -0.5, ($R^2 = 0,93$), R = 0.8.
Harris
 CLD
 R = -0,5, S-
Kawai,
Boerstra, S-N R=-0.5, S-N
Kassapoglou

➤
Boerstra **Harris, Kawai**
Kassapoglou
 CLD
Harris, **Kawai**
 10^5 #3. **Harris**, **Boerstra**
 R = 0,8 R = -0,5 **Kawai**
Kassapoglou, S-
Kawai

Table 1

Comparison of predicting ability of the applied models in terms of the coefficient of multiple determination (R^2).

	Material #1	Material #2		Material #3		
	$R = 0.5$	$R = -0.4$	$R = -2.5$	$R = -1$	$R = -0.5$	$R = 0.8$
Linear	0.37	0.72	0.61	-	0.93	0.35
Piecewise linear	0.89	0.91	0.84	-	0.88	0.93
Harris-f: linear	0.63	0.95	0.71	-	0.77	0.51
Harris-f: power law	0.64	0.94	0.64	-	0.94	0.80
Kawai ($R = -1$)	0.15	0.94	0.83	-	0.87	0.31
Kawai ($R = -0.5$)	-	-	-	0.76	-	0.43
Boerstra- experimental data	0.65	0.86	0.83	-	0.60	0.85
Boerstra-S-N data	0.69	0.89	0.84	-	0.84	0.91
Kassapoglou	-	-	-	0.93	0.41	0.48

CLD

(Kawai)

(Harris Boerstra).

Kassapoglou

Kawai.

S- Goodman,

Harris Boerstra.

Harris, Kawai Boerstra, Kassapoglou.

CLD

(log-logS-)

CLD.

S- S-

CLD

#2

μ

S-

μ

50%

95%

μ

μ

μ

μ

S-

μ

10^3

10^7

μ

μ

LCD,

μ

μ

S-

μ

μ

μ

μ

$\mu\mu$

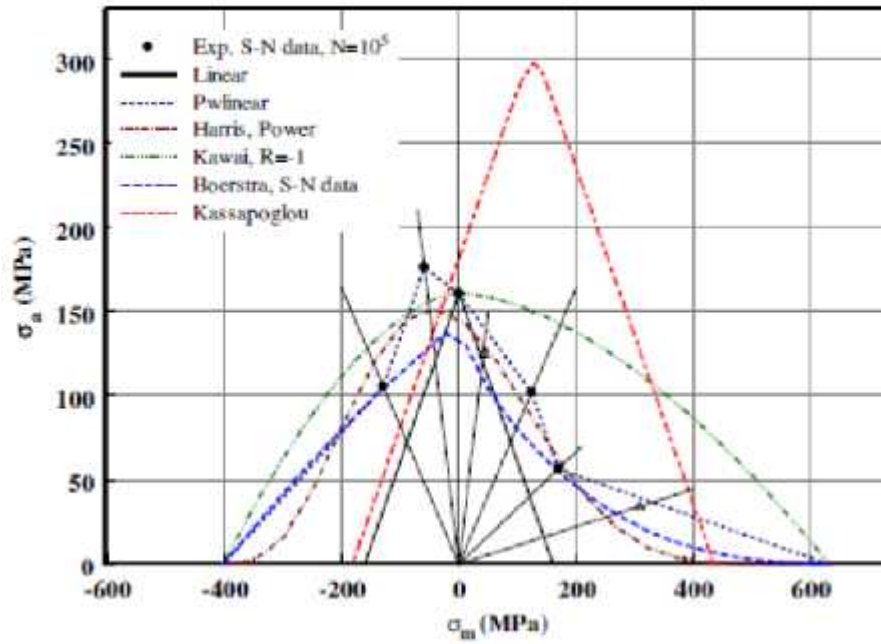


Fig. 5. Comparison of CL lines for 10^5 cycles, material #3.

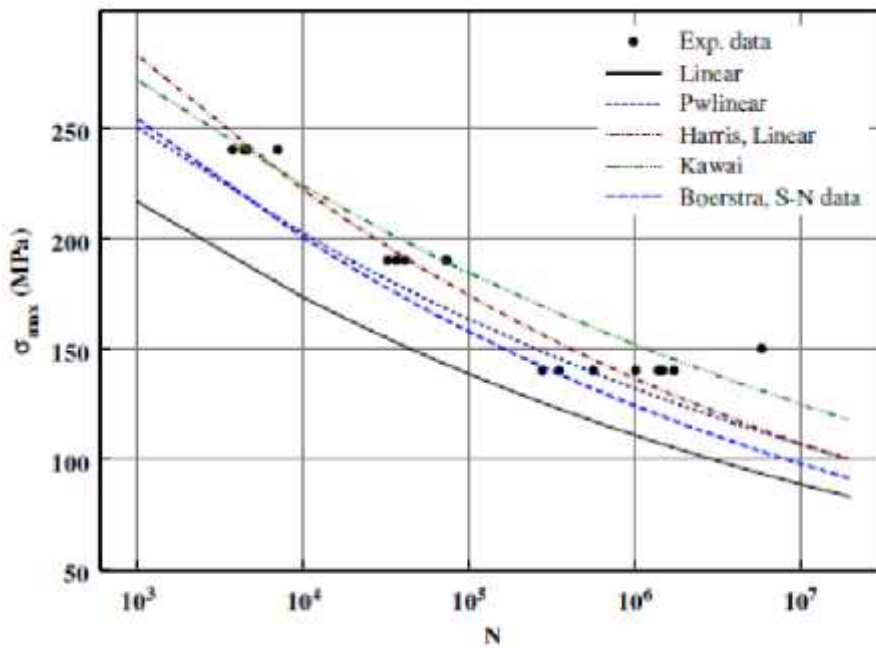


Fig. 7. Predicted S-N curves for $R = -0.4$, material #2.

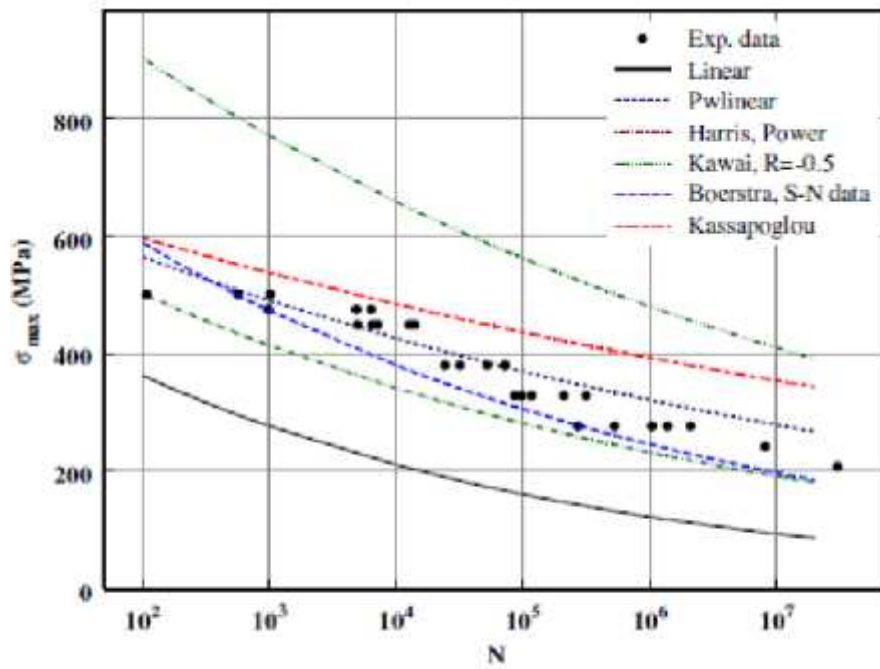


Fig. 8. Predicted S-N curves for $R = 0.8$, material #3.

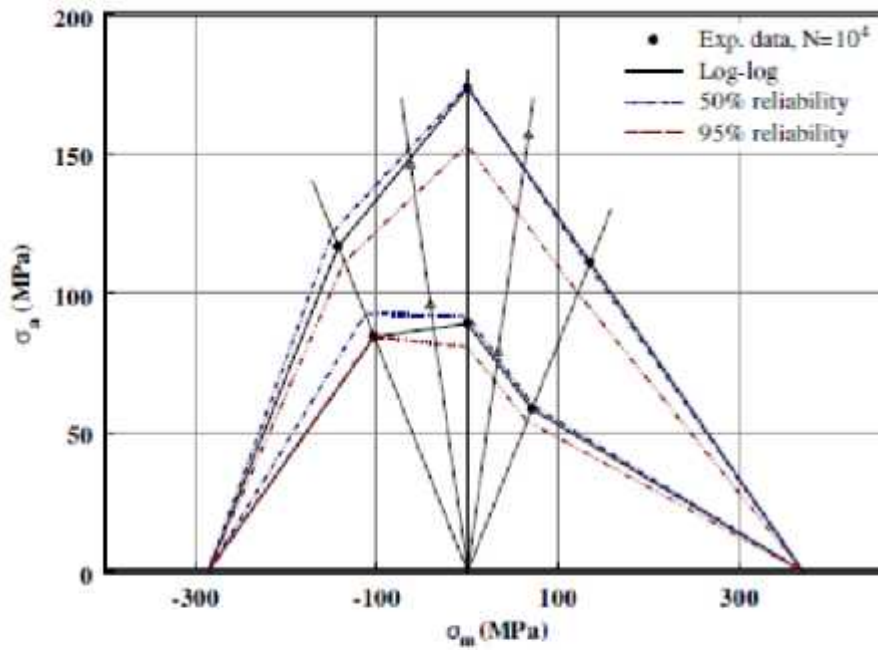


Fig. 9. Comparison of CLDs based on different S-N formulations and different reliability levels, material #2.

μ μ
 μ μ μ μ
 μ μ μ μ μ
 μ μ μ μ μ μ
 μ μ μ μ μ μ μ

GFRP.

• **CLD** (Continuous Length Distribution) is a type of CLD. It is characterized by a distribution that is continuous and unimodal. The distribution is often used to describe the length distribution of fibers in a composite.

• The relationship between $R = 1$ and the S-N curve is often used to determine the strength of a composite. For $R = 1$, the S-N curve is often used to determine the strength of a composite. The relationship between $R = 1$ and the S-N curve is often used to determine the strength of a composite.

• **Harris** and **Kawai** are two models used to describe the strength of a composite. **Harris** is a model that is based on the Weibull distribution, while **Kawai** is a model that is based on the GFRP (Glass Fiber Reinforced Plastic) model.

• **Kawai** is a model that is based on the GFRP (Glass Fiber Reinforced Plastic) model. It is used to describe the strength of a composite. The relationship between $R = 1$ and the S-N curve is often used to determine the strength of a composite.

• **GFRP** (Glass Fiber Reinforced Plastic) is a type of composite. It is characterized by a distribution that is continuous and unimodal. The distribution is often used to describe the length distribution of fibers in a composite.

• **Harris** is a model that is based on the Weibull distribution. It is used to describe the strength of a composite. The relationship between $R = 1$ and the S-N curve is often used to determine the strength of a composite.

• **Boerstra** is a model that is based on the Weibull distribution. It is used to describe the strength of a composite. The relationship between $R = 1$ and the S-N curve is often used to determine the strength of a composite.

• **Boerstra** is a model that is based on the Weibull distribution. It is used to describe the strength of a composite. The relationship between $R = 1$ and the S-N curve is often used to determine the strength of a composite.

4.7

• The relationship between T_g and the S-N curve is often used to determine the strength of a composite. For $T_g > 3$, the S-N curve is often used to determine the strength of a composite.

• The relationship between $R = 1$ and the S-N curve is often used to determine the strength of a composite. For $R = 1$, the S-N curve is often used to determine the strength of a composite.

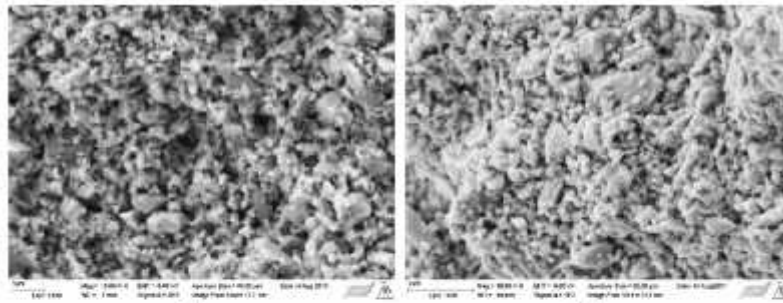
• The relationship between $R = 1$ and the S-N curve is often used to determine the strength of a composite. For $R = 1$, the S-N curve is often used to determine the strength of a composite.

• The relationship between $R = 1$ and the S-N curve is often used to determine the strength of a composite. For $R = 1$, the S-N curve is often used to determine the strength of a composite.

max μ μ (max) μ μ .
 μ μ μ . μ max μ μ μ μ μ
 , μ μ μ Piola-Kirchhoff μ μ , μ μ μ μ
 μ μ μ μ Poisson μ , μ μ μ .
 μ μ 50 pph SA μ μ μ r μ
 μ 50 pph SBR, SA μ μ Young SA μ
 SBR, μ μ Tg. μ SBR. g1
 SA μ SA 5 pph. SA μ SA 50 pph,
 ' μ SBR μ . SA μ μ 1, UT
 SA μ μ 50 pph μ μ μ μ SBR.
 μ (PVC) , μ μ (CPVC)
 μ μ μ μ μ μ CPVC
 μ μ , μ μ μ μ μ μ μ .
 CPVC μ μ PVC μ .
 SA SBR μ μ μ μ g1
 10 pph 10 pph . μ μ .
 CPVC.

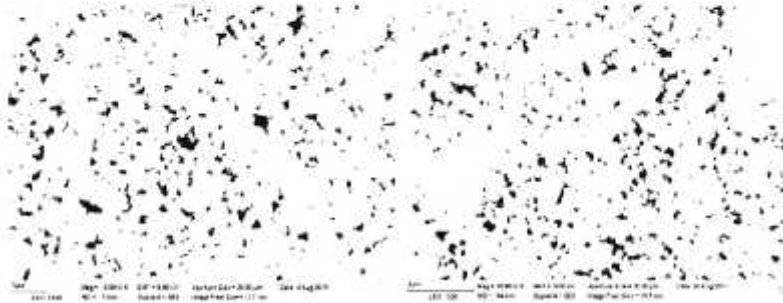
Table 2
 Summary of fatigue life behaviour for each composite tested. The gradient of the logarithmic maximum cyclic stress plots is denoted by m . Numbered subscripts for σ , P and m relate to the cycles upon which this data is based.

Polymer	SEB																											
	5A			10			5			50			10			5												
pph	50	10	5	50	10	5	50	10	5	50	10	5	50	10	5	50	10	5										
ϵ_s (mstrain)	28.0	16.6	11.1	5.5	2.1	1.4	0.7	1.1	1.7	1.1	0.7	1.4	1.0	0.7	0.6	59.5	41.6	31.1	15.0	2.0	1.5	1.0	0.5	1.3	1.0	0.8	0.6	
ϵ_r (%)	28.6	17.0	11.3	5.6	42.4	34.2	22.9	13.2	42.4	31.4	20.9	18.7	41.0	28.6	21.5	10.3	45.1	33.2	22.1	11.2	50.1	37.5	22.1	11.2	50.1	37.5	31.1	22.5
N_f	2	110	3500	17,000	30	100	1000	41,500	40	900	2,000	15,000	7	50	600	18,000	6	300	3500	24,000	30	400	2000	30	400	2000	2500	2500
σ_{max} (MPa)	24.39	34.21	31.68	20.74	11.36	12.29	8.08	4.69	8.03	6.07	4.62	4.13	13.55	6.70	10.73	8.84	12.75	11.41	8.07	4.79	5.84	4.56	4.79	5.84	4.56	3.56	1.07	
σ_{10} (MPa)	-	15.88	16.37	12.92	8.72	9.92	7.25	4.47	6.37	5.15	4.00	3.74	-	3.11	5.23	5.53	-	9.63	7.14	4.42	4.49	3.93	3.05	4.49	3.93	3.05	0.66	
σ_{100} (MPa)	-	7.01	8.21	7.89	-	-	6.97	4.21	-	4.79	3.92	3.51	-	-	2.76	3.39	-	8.88	6.67	4.33	-	3.62	2.97	4.33	3.62	2.97	0.31	
m_{2-100}	-	-4.56	-3.8	-2.25	-0.54	-0.41	-0.17	-0.09	-0.36	-0.2	-0.11	-0.1	-2.87	-0.86	-1.20	-0.94	-2.1	-0.37	-0.23	-0.06	-0.22	-0.13	-0.07	-0.22	-0.13	-0.07	-0.14	
g_1 (GPa)	-	2.06	2.85	3.77	5.41	7.23	7.35	6.7	5.73	6.07	6.6	6.88	0.23	0.16	0.35	0.59	6.38	7.61	8.07	9.58	4.49	4.56	4.45	4.49	4.56	4.45	1.78	
P_2	-	0.44	0.24	0.23	0.22	0.18	0.09	0.07	0.17	0.11	0.08	0.10	0.70	0.71	0.71	0.70	0.18	0.13	0.11	0.07	0.16	0.11	0.11	0.16	0.11	0.11	0.14	
P_{10}	-	0.50	0.42	0.31	0.27	0.23	0.09	0.07	0.20	0.17	0.11	0.09	-	0.69	0.70	0.69	-	0.15	0.11	0.08	0.17	0.13	0.12	0.17	0.13	0.12	0.12	
P_{100}	-	0.54	0.48	0.35	-	-	0.11	0.08	-	0.18	0.11	0.10	-	-	0.64	0.65	-	0.15	0.12	0.09	-	0.14	0.12	0.09	-	0.14	0.12	0.09



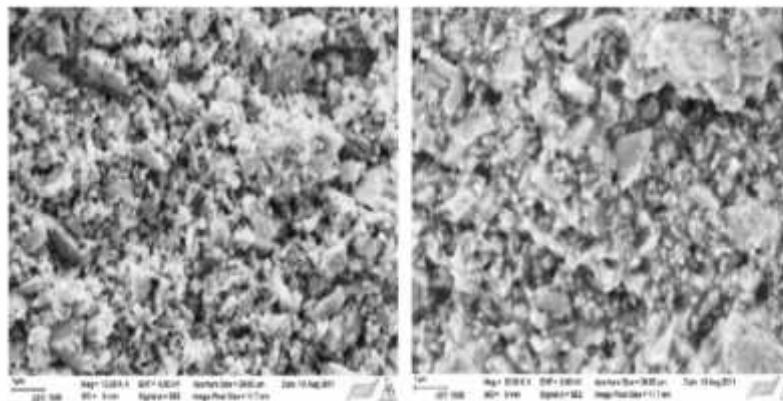
(a)

(b)



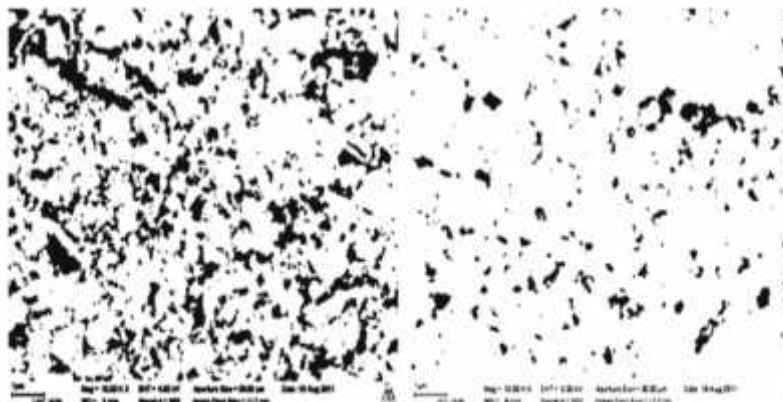
(c)

(d)



(a)

(b)



(c)

(d)

μ GCC μ μ μ μ
 μ PV_F μ SA SA μ μ μ μ
 μ SA SA μ μ μ SBR. μ
 μ SA SBR μ SA μ
 μ μ μ μ μ μ μ μ
 μ μ μ μ μ μ μ

Table 3
Summary of results.

Polymer	pph	Maximum ϵ_0 tested			Minimum ϵ_0 tested		
		ϵ_r (%)	N_f	P_{10}	ϵ_r (%)	N_f	P_{10}
SA	50	28.6	2	-	5.6	17,000	0.31
	10	42.4	30	0.27	13.2	41,500	0.07
	5	42.4	40	0.20	18.7	15,000	0.09
SBR	50	41	7	-	10.3	18,000	0.69
	10	45.1	6	-	11.2	24,000	0.08
	5	50.1	30	0.17	22.5	2500	0.12

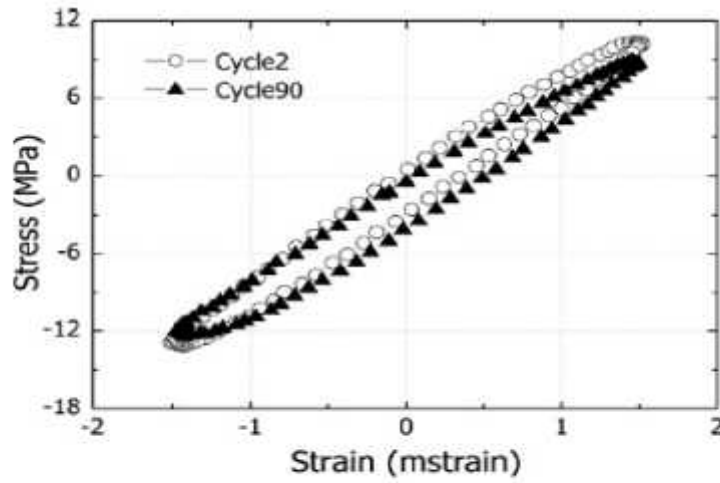


Fig. 5. Hysteresis loops from 10 pph SBR polymer-pigment composite at 1.0 mstrain amplitude.

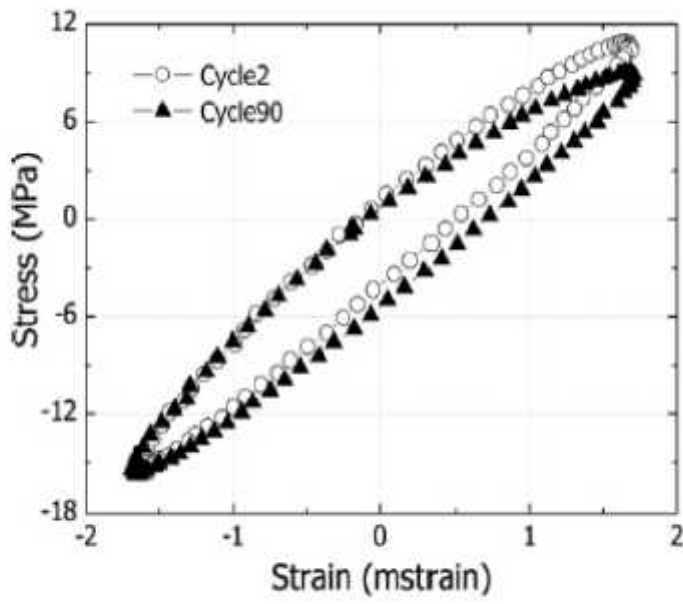


Fig. 6. Hysteresis loops from 10 pph SA polymer-pigment composite at 1.1 mstrain amplitude.

SBR SA 10pph. max
 SBR. SA
 SBR. SA

... T_g ...
 ... 3. ... (5 pph) ... (50 pph)
 ... 10 pph ...
 ... PVF₂ ...
 SA. ... 10 pph ...
 ...

4.8 / μ - μ

...
 ... ().
 ... S-
 ...
 ...
 ... ().
 ...
 ...
 ...
 ...
 ...
 ...
 ... 200 C.
 ...
 « μ - μ »
 ...

The loading curve shows a linear relationship between stress and strain up to approximately 85 MPa, after which the material exhibits non-linear behavior. The unloading curve shows a hysteresis loop, with the permanent strain being approximately 2500 $\mu\epsilon$ at a maximum stress of 85 MPa. The permanent strain is approximately 85% of the total strain at the maximum stress.

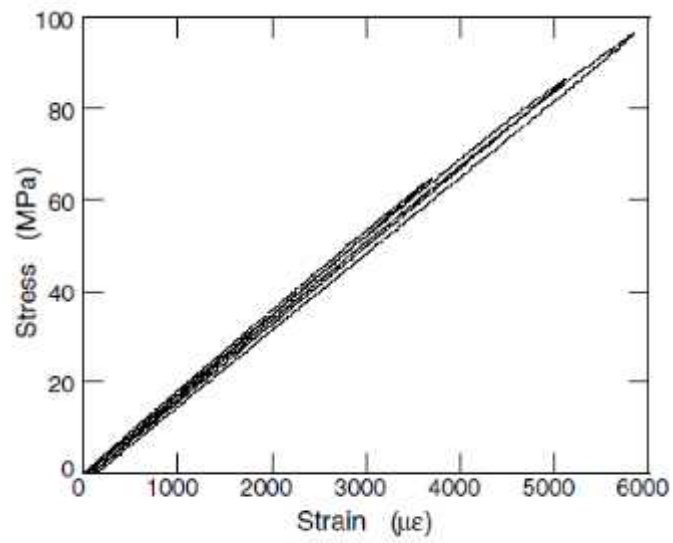


Fig. 1. Loading/unloading stress–strain curve of a GF/phenol composite.

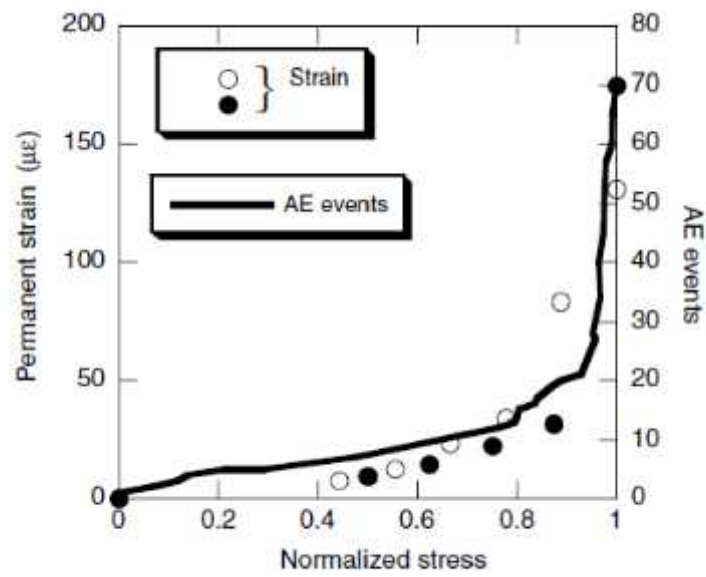
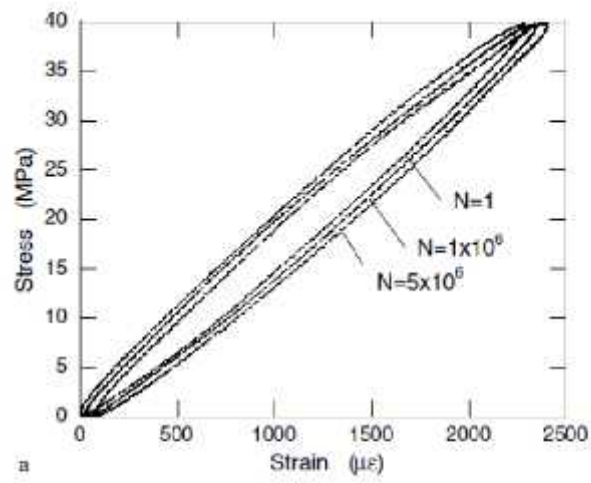


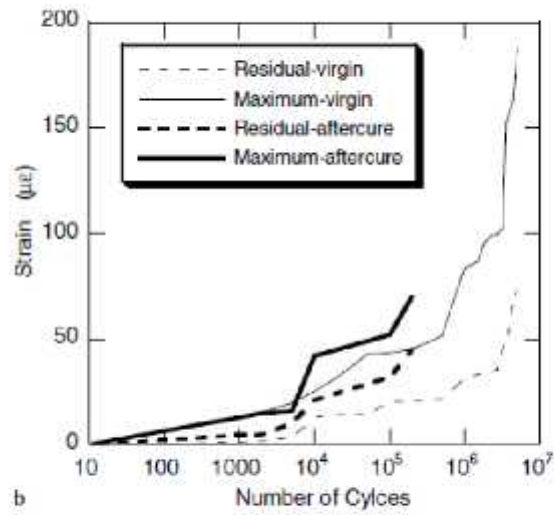
Fig. 2. Permanent strain and cumulative AE events during tensile loading.

μ 6
μ μ
μ
μ

μ μ μ μ μ μ
μ μ μ μ μ μ
μ μ μ μ μ μ



a



b

Fig. 4. Change in the: (a) stress-strain curves for the virgin specimen, and (b) maximum and residual strain increments for the virgin and long-term after-cured specimens during fatigue loading at maximum stress of 40 MPa.

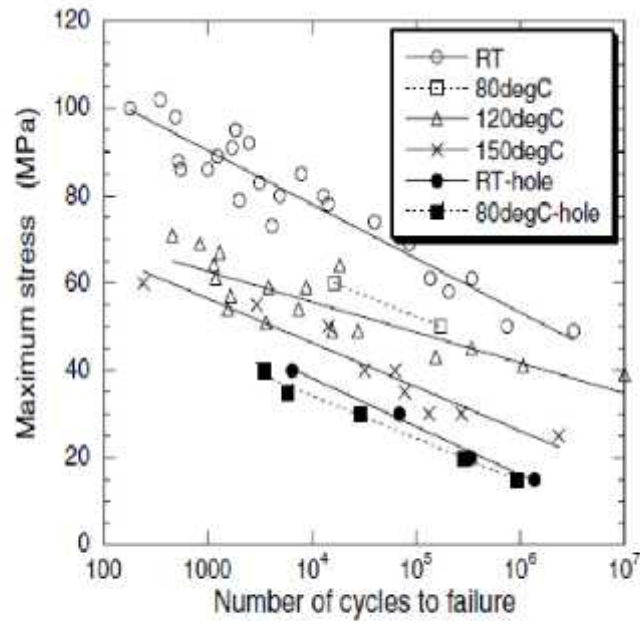


Fig. 5. Effect of temperature on *S-N* curves of the specimen with and without a hole.

Table 2
The slope of *S-N* curves *b* at various temperatures

Temperature (°C)	Hole	<i>b</i> (MPa)
25 (RT)	N	12.36
80	N	9.80
120	N	6.99
150	N	10.10
25 (RT)	Y	11.08
80	Y	9.81

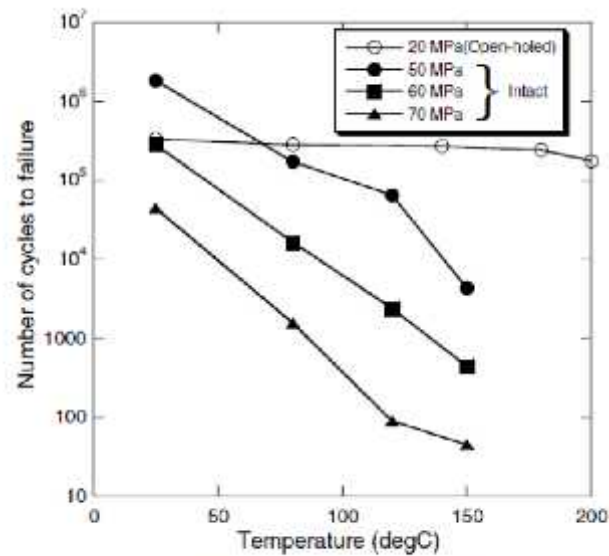


Fig. 6. Effect of temperature on number of cycles to failure of intact and open-holed specimens.

μ 7 μ μ μ μ μ μ μ μ μ
 μ 8 μ μ μ μ μ μ μ μ μ μ μ μ μ μ μ
 μ 9 μ μ μ μ μ μ μ μ μ μ μ μ μ μ μ μ μ (200 C/100 h)
 μ
 μ
 μ 10 μ
 μ
: () 20° C, 20MPa, () 180° C, 20 MPa, () 200° C, 20 MPa, () 20° C, 15 MPa, () 20° C, 40 MPa
() $3,33 \cdot 10^5$, () $2,43 \cdot 10^5$, () $1,75 \cdot 10^5$, () $1,37 \cdot 10^6$, () $6,48 \cdot 10^3$.
 μ 180 C. μ μ μ μ μ μ μ μ μ μ μ μ μ μ μ μ μ μ μ
() () μ () μ () μ () μ () μ () μ
 μ () () μ () μ () μ () μ () μ () μ

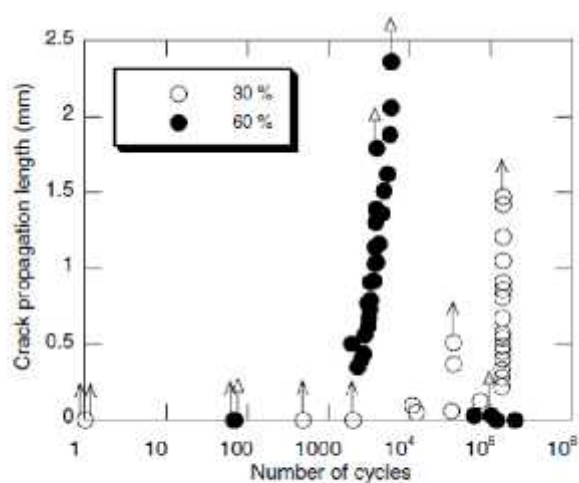


Fig. 7. Crack propagation length in the FCP tests. The arrows denote final fracture.

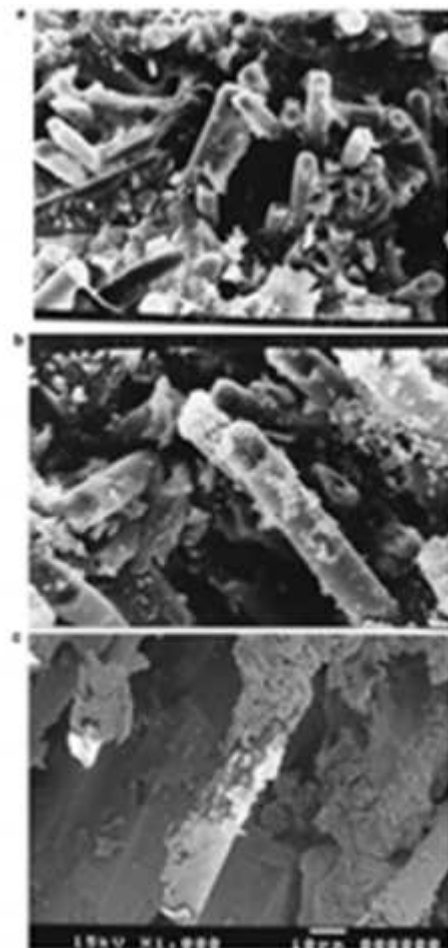


Fig. 8. Fracture surface of the Zn virgin specimens after monotonic tensile test, (a) virgin, and (b) long-term after-cured (200°C/100h) specimens after fatigue tests. The number of cycles to failure and maximum stress are (a) $1.67 \cdot 10^5$, 30 MPa and (c) $2.50 \cdot 10^5$, 40 MPa.

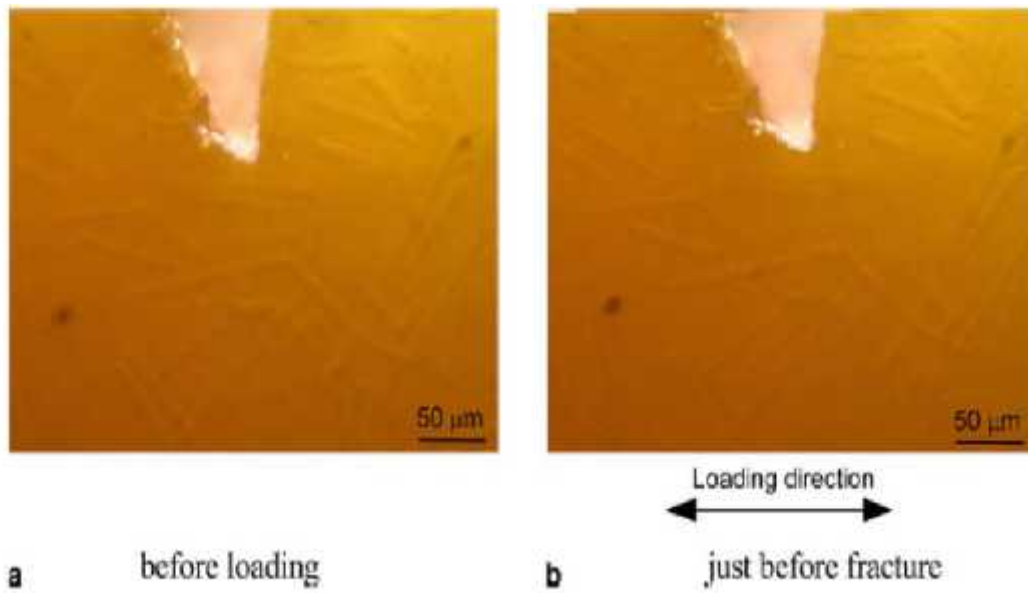


Fig. 8. In situ optical micrographs showing notch tips before loading and just before fracture.

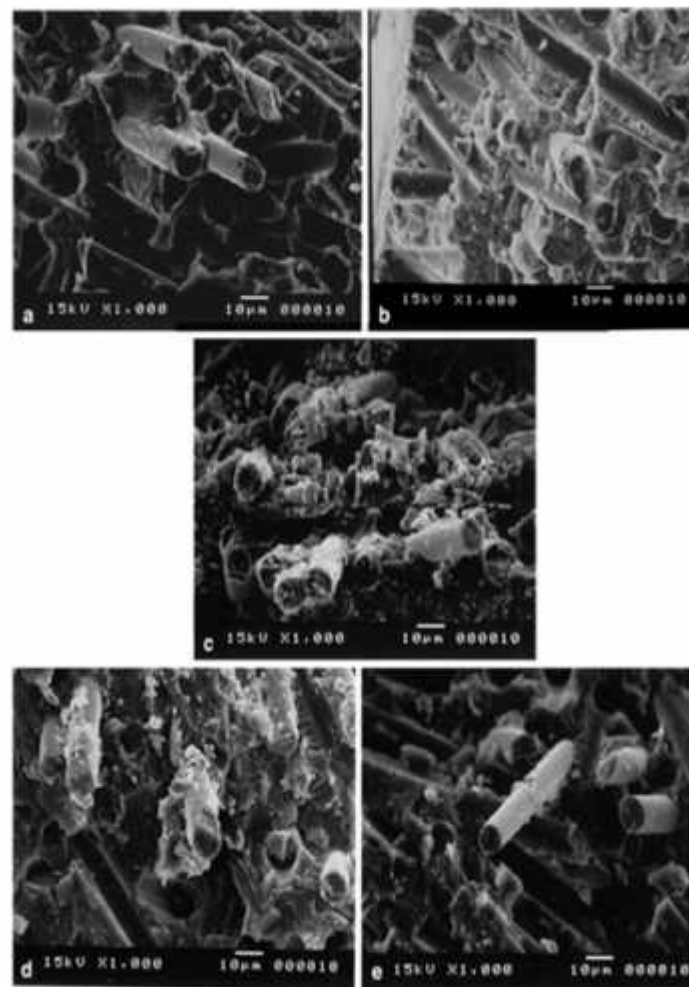


Fig. 10. Fracture surfaces of open-holed specimens after fatigue tests at temperature and maximum stress of: (a) 20 °C, 20 MPa, (b) 180 °C, 20 MPa, (c) 200 °C, 20 MPa, (d) 20 °C, 15 MPa, and (e) 20 °C, 40 MPa. The number of cycles to failure is (a) 3.33×10^6 , (b) 2.43×10^6 , (c) 1.75×10^6 , (d) 1.37×10^6 and (e) 6.48×10^5 .

5.

1. [www.fiberglast.com](#), μ, μ μ μ «
2. Ever J. Barbedo, «Introduction to Composite Materials Design»
3. www.science@direct.com
4. Forbes Aird, «Fiberglass and Composite Materials»
5. Andrew Marshall, «Composite Basics»
6. John J. Morena, «Advanced Composite Moldmaking»
7. K. Diamanti, C. Soutis and J.M. Hodgkinson, «Non-destructive inspection of sandwich and repaired composite laminated structures » , (Composites Science and Technology, Volume 65, Issue 13, October 2005, Pages 2059-2067)
8. C. Soutis, «Carbon fiber reinforced plastics in aircraft construction» (Materials Science and Engineering: A, In Press, Corrected Proof
9. C. Soutis, «Fibre reinforced composites in aircraft construction», (Progress in Aerospace Sciences, Volume 41, Issue 2, February 2005, Pages 143-151)
10. Maria Kashtalyan and Costas Soutis, «Analysis of composite laminates with intra- and interlaminar damage », (Progress in Aerospace Sciences, Volume 41, Issue 2, February 2005, Pages 152-173)
11. K. Diamanti, C. Soutis and J.M. Hodgkinson, «Lamb waves for the non-destructive inspection of monolithic and sandwich composite beams» (Composites Part A: Applied Science and Manufacturing, Volume 36, Issue 2, February 2005, Pages 189-195)
12. J. Lee and C. Soutis, «Thickness effect on the compressive strength of T800/924C carbon fibre-epoxy laminates » (Composites Part A: Applied Science and Manufacturing, Volume 36, Issue 2, February 2005, Pages 213-227)
13. Koundouros, Brian G. Falzon, Costas Soutis and Steven J. Lord, «Predicting the ultimate load of a CFRP wingbox» (Composites Part A: Applied Science and Manufacturing, Volume 35, Issues 7-8, July 2004, Pages 895-903)
14. Maria Kashtalyan and Costas Soutis, «Analysis of local delaminations in composite laminates with angle-ply matrix cracks» (International Journal of Solids and Structures, Volume 39, Issue 6, March 2002, Pages 1515-1537)
15. Seth S. Kessler, S. Mark Spearing, Mauro J. Atalla, Carlos E. S. Cesnik and Constantinos Soutis, «Damage detection in composite materials using frequency response methods » (Composites Part B: Engineering, Volume 33, Issue 1, January 2002, Pages 87-95)
16. Y. Zhuk, I. Guz and C. Soutis, «Compressive behaviour of thin-skin stiffened composite panels with a stress raiser » (Composites Part B: Engineering, Volume 32, Issue 8, December 2001, Pages 697-709)
17. Costas Soutis and Igor A. Guz, «Predicting fracture of layered composites caused by internal instability», (Composites Part A: Applied Science and Manufacturing, Volume 32, Issue 9, September 2001, Pages 1243-1253)
18. V. J. Hawyes, P. T. Curtis and C. Soutis, «Effect of impact damage on the compressive response of composite laminates», (Composites Part A: Applied Science and Manufacturing, Volume 32, Issue 9, September 2001, Pages 1263-1270)
19. www.fiberglast.com
20. www.mdacomposites.org
21. www.e-composites.com
22. www.reichhold.com
23. www.tencom.com
24. www.fulcrumcomposites.com
25. www.wikipedia.org